

proton and complex formation with functionalized cyclodextrins. These results confirm, as we have already reported,^{45,54,65} that a combined spectroscopic and thermodynamic approach is very useful to infer structural information on the investigated species. In fact, through the NMR investigation it is possible to describe the conformational features of the initial and final states of the different species present in the system (these states determine thermodynamic parameters), and therefore, it is possible to know the role of the cavity in determining a peculiar structure of the complex species. The EPR results give evidence of the interaction with the cavity through the comparison between the magnetic parameters of the two mono complexes [Cu(CDhm)]²⁺ and [Cu(hm)]²⁺ and substantiate the smaller entropy value found for the former. The inclusion of the imidazole ring in the mono- and

diprotonated species underlines the inclusion properties of the cyclodextrin cavity. It has been previously found that the protonation of a basic center removes the residue, as imidazole, from a hydrophobic center.⁶⁶ Thus, the unexpected promotion of inclusion due to the imidazole protonation is a finding that can contribute to the debate about the exact nature of binding interaction⁶⁷ and the description of the cyclodextrin cavity as a simply hydrophobic site.⁶⁰

Acknowledgments. We thank the CNR (Rome) for partial support of this work (PF Chimica Fine II). We also thank Prof. I. Bertini (University of Florence—Servizio Nazionale di Risonanza Magnetica Nucleare) for the NMR facilities.

(65) Arena, G.; Bonomo, R. P.; Impellizzeri, G.; Izatt, R. M.; Lamb, J. D.; Rizzarelli, E. *Inorg. Chem.* 1987, 26, 785.

(66) Arena, G.; Impellizzeri, G.; Maccarrone, G.; Pappalardo, G.; Sciotto, D.; Rizzarelli, E. *Thermochim. Acta* 1989, 154, 97.

(67) Bergeron, R. J. In *Inclusion Compounds*; Davies, J. E. D., MacNicol, D. D., Eds.; Academic Press: London, 1984; Vol. 3, p 391.

Contribution from the Chemistry Departments, The Ohio State University, Columbus, Ohio 43210, The University of Kansas, Lawrence, Kansas 66045, and University of Warwick, Coventry CV4 7AL, England

Sterically Hindered Nickel(II) and Iron(II) Lacunar Cyclidene Complexes Containing *gem*-Dimethyl Groups on Their Saturated Chelate Rings

Peter A. Padolik, Alan J. Jircitano, Nathaniel W. Alcock, and Daryle H. Busch*

Received July 13, 1990

The structure of the cyclidene ligand in the corresponding iron(II)-centered dioxygen carrier has been altered by the addition of *gem*-dimethyl groups to increase the bulk on the saturated rings of the parent macrocycle. Dramatic responses are found in the dioxygen affinities of the resulting complexes. Placing the bulky group to the rear of the cavity, within which the O₂ binds, enhances the O₂ affinity, while placing the group at the entry greatly decreases the affinity. The presence of bulky groups at both positions essentially stops the binding of O₂. Interpretations are based on the crystal structure data and molecular modeling. X-ray structure data for [DMNiDM(Me₂Me₂Mxyl)[16]cyclidene](PF₆)₂: NiC₃₂H₄₈N₆O₂F₁₂, monoclinic, *P*₂₁/*c*, *a* = 13.541 (4) Å, *b* = 15.408 (5) Å, *c* = 20.471 (7) Å, β = 106.10°, *V* = 4103 (2) Å³, *Z* = 4, *R* = 0.083, and *R*_w = 0.091 for 3302 reflections with *I* > 2.0σ.

Introduction

Steric bulk is of major significance in the functioning of the dioxygen carriers of nature and the few well-characterized synthetic iron(II) dioxygen carriers. In the globular proteins of myoglobin and hemoglobin the mass of the protein prevents two iron(II) atoms from simultaneously binding to a single O₂ molecule. In the T-form of hemoglobin, a valine residue effectively blocks the O₂ binding site of the β-subunits.¹ The selection between O₂ and CO at the hemoglobin and myoglobin binding sites is affected by the nearest protein residues on the distal side of the porphyrin ring.² Many investigators,³ beginning with Baldwin et al.⁴ and Collman et al.,⁵ have built superstructures on porphyrins to provide the same steric protection provided by the proteins of the natural products. Steric effects have been pursued at greater length by Traylor et al.⁶ In these laboratories, the totally synthetic lacunar cyclidene ligands (Figure 1) utilize similar superstructures to stabilize their dioxygen adducts.⁷ The cobalt(II) cyclidene complexes constitute a large family of highly efficacious dioxygen carriers whose O₂ affinities are readily fine-tuned by small incremental changes in the size of the O₂-accommodating cavity.⁸ A relatively small group of the iron(II) cyclidene complexes comprise the only well-characterized non-porphyrin synthetic, heme-protein-model dioxygen carriers based on iron(II).⁹ In general a *m*-xylylene roof to the cyclidene cavity will provide the necessary shielding of the binding site to produce reversible O₂ binding. However, the *m*-xylylene-bridged complex is remarkably sensitive to the steric bulk of other substituents in the structure. For example, replacing the methyl groups at the R² and R³ positions of Figure 1 with the bulky groups phenyl and benzyl, respectively, retards the rate of air oxidation of the oxygen

carrier by about 4 orders of magnitude. In a very real sense this increased bulk is at the periphery of the structure but adjacent

- (1) (a) Perutz, M. F. *Nature (London)* 1970, 228, 726. (b) Perutz, M. F.; Fermi, G.; Luisi, B.; Shaanan, B.; Liddington, R. C. *Acc. Chem. Res.* 1987, 20, 309. (c) Brzozowski, A.; Derewenda, Z.; Dodson, E.; Dodson, G.; Glabowski, M.; Liddington, R.; Skarzynski, T.; Vallely, D. *Nature (London)* 1984, 307, 74.
- (2) (a) Antonini, E.; Brunori, M. *Hemoglobin and Myoglobin and their Reaction with Ligands*; Elsevier: New York, 1971; p 93. (b) Collman, J. P.; Brauman, J. I.; Halbert, R. R.; Suslick, K. S. *Proc. Natl. Acad. Sci. U.S.A.* 1976, 73, 3333. (c) Collman, J. P.; Brauman, J. I.; Doxsee, K. M. *Proc. Natl. Acad. Sci. U.S.A.* 1979, 76, 6035. (d) Geibel, J.; Cannon, J.; Campbell, D.; Traylor, T. G. *J. Am. Chem. Soc.* 1978, 100, 3575. (e) Traylor, T. G. *Acc. Chem. Res.* 1981, 14, 102.
- (3) (a) Meade, T. J.; Busch, D. H. *Prog. Inorg. Chem.* 1985, 33, 59. (b) Baldwin, J. E.; Crossley, M. J.; Klose, T.; O'Rear, E. A.; Peters, M. K. *Tetrahedron* 1982, 38, 27. (c) Traylor, T. G.; Mitchell, M. J.; Tsuchiya, S.; Campbell, D. H.; Stunes, D. V.; Koga, N. J. *J. Am. Chem. Soc.* 1981, 103, 5234. (d) Traylor, T. G.; Koga, N.; Deardurff, L. A.; Swepston, P. N.; Ibers, J. A. *J. Am. Chem. Soc.* 1984, 106, 5132. (e) Chang, C. K. *J. Am. Chem. Soc.* 1977, 99, 2819. (f) Collman, J. P.; Brauman, J. I.; Collins, T. J.; Iverson, B. R.; Lang, G.; Pettman, R. G.; Sessler, J. L.; Walters, M. A. *J. Am. Chem. Soc.* 1983, 105, 3083. (g) Mometeau, M.; Lavalette, D. *J. Chem. Soc., Chem. Commun.* 1982, 341.
- (4) Almog, J.; Baldwin, J. E.; Huff, J. *J. Am. Chem. Soc.* 1975, 97, 227.
- (5) (a) Collman, J. P.; Gagne, R. R.; Halbert, T. R.; Marchon, T. R.; Reed, J. C. *J. Am. Chem. Soc.* 1973, 95, 7868. (b) Collman, J. P. *Acc. Chem. Res.* 1977, 10, 265.
- (6) (a) Traylor, T. G.; Taube, D. J.; Jongeward, K. A.; Magde, D. *J. Am. Chem. Soc.* 1990, 112, 6875. (b) Traylor, T. G.; Koga, N.; Deardurff, L. A. *J. Am. Chem. Soc.* 1985, 107, 6504.
- (7) (a) Busch, D. H.; Stephenson, N. A. *J. Inclusion Phenom. Mol. Recognit. Chem.* 1989, 7, 137. (b) Busch, D. H. *La Trasfusione del Sangue* 1988, 1, 57. (c) Busch, D. H. In *Oxygen Complexes and Oxygen Activation by Transition Metals*; Martell, A. E., Sawyer, D. T., Eds.; Plenum: New York, 1988; p 61. (d) Busch, D. H.; Cairns, C. In *Progress in Macrocyclic Chemistry*; Izatt, R. M., Christensen, J. J., Eds.; Wiley-Interscience: New York, 1987; p 1. (e) Cairns, C. J.; Busch, D. H. *Inorg. Synth.* 1990, 27, 261.

* To whom correspondence should be addressed at The University of Kansas.

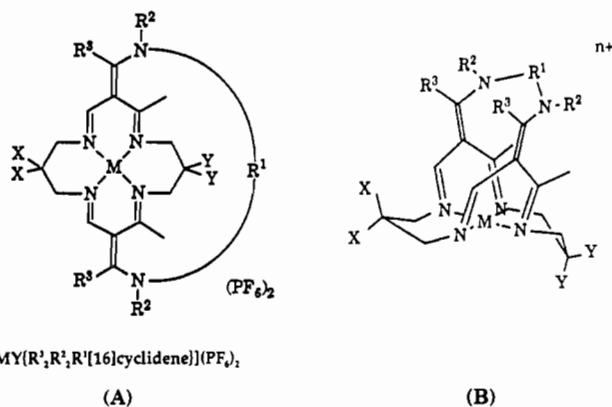
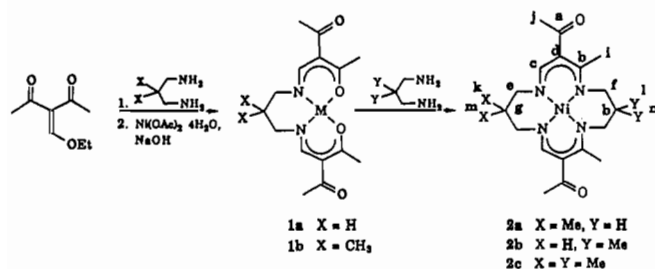
[XMY(R¹,R²,R³)[16]cyclidene)](PF₆)₂

Figure 1. Structures of complexes of the substituted cyclidene ligands: (A) flat projection; (B) three-dimensional image. Compound key: (a) X = Me, Y = H, R² = R³ = Me; (b) X = H, Y = Me, R² = R³ = Me; (c) X = Me, Y = Me, R² = R³ = Me; (d) X = Me, Y = H, R² = PhCH₂, R³ = Ph; (e) X = H, Y = Me, R² = PhCH₂, R³ = Ph; (f) X = Me, Y = Me, R² = PhCH₂, R³ = Ph.

Scheme I



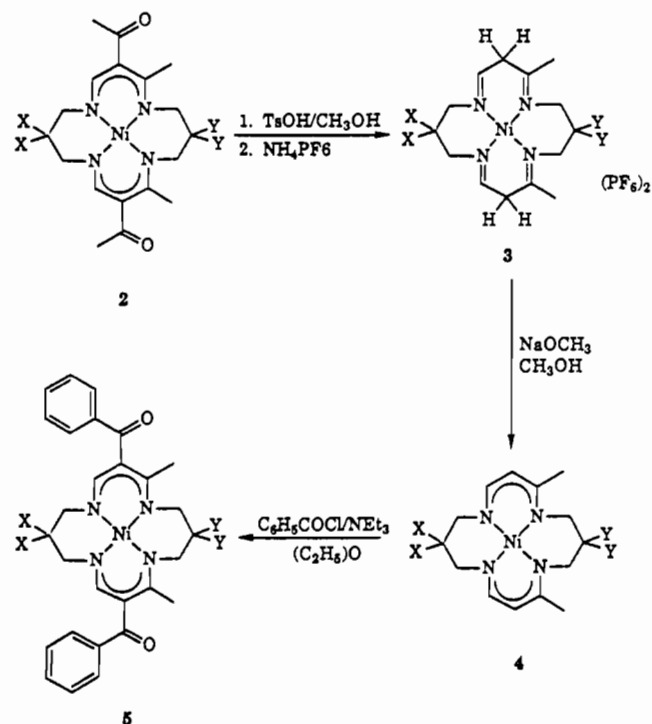
to the entries into the cavity that must accommodate the guest O₂ molecule. Consequently, the exploration of the effects of increased bulk at other locations peripheral to the cavity is a matter of considerable importance. We report here the influence of inserting bulky *gem*-dimethyl groups into the structures of the *m*-xylylene-bridged complexes of nickel(II) and iron(II). These groups are so intimately associated with the metal binding sites that they greatly affect the ability of that ion to bind the fifth and sixth ligands.

Results

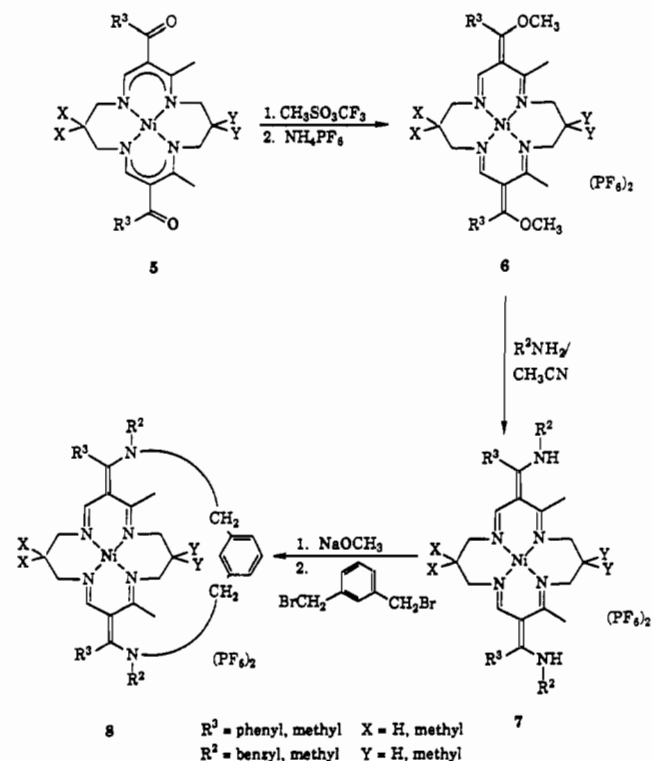
Synthesis of the Nickel(II) Complexes and Ligand Salts. Six new cyclidene ligands are reported here along with their nickel(II) and iron(II) complexes. The new ligands are prepared by a series of reactions, mostly using the nickel(II) complexes, yielding four-coordinate, square-planar nickel(II) cyclidene complexes. The ligands are then removed from the nickel and coordinated to

- (8) (a) Stevens, J. C.; Jackson, P. J.; Schammel, W. P.; Christoph, G. G.; Busch, D. H. *J. Am. Chem. Soc.* **1980**, *102*, 3283. (b) Stevens, J. C.; Busch, D. H. *J. Am. Chem. Soc.* **1980**, *102*, 3285. (c) Herron, N.; Chavan, M. Y.; Busch, D. H. *J. Chem. Soc., Dalton Trans.* **1984**, 1491. (d) Goldsby, K. A.; Meade, T. J.; Kojima, M.; Busch, D. H. *Inorg. Chem.* **1985**, *24*, 2588. (e) Cameron, J. H.; Kojima, M.; Korybut-Daszkiwicz, B.; Coltrain, B. K.; Meade, T. J.; Alcock, N. W.; Busch, D. H. *Inorg. Chem.* **1987**, *26*, 427. (f) Meade, T. J.; Takeuchi, K. J.; Busch, D. H. *J. Am. Chem. Soc.* **1987**, *109*, 725. (g) Hoshino, N.; Jircitano, A.; Busch, D. H. *Inorg. Chem.* **1988**, *27*, 2292. (h) Thomas, R.; Fendrick, C. M.; Lin, W.-K.; Glogowski, M. W.; Chavan, M. Y.; Alcock, N. W.; Busch, D. H. *Inorg. Chem.* **1988**, *27*, 2534. (i) Tweedy, H. E.; Alcock, N. W.; Matsumoto, N.; Padolik, P. A.; Stephenson, N. A.; Busch, D. H. *Inorg. Chem.* **1990**, *29*, 616.
- (9) (a) Herron, N.; Busch, D. H. *J. Am. Chem. Soc.* **1981**, *103*, 1236. (b) Herron, N.; Cameron, J. H.; Neer, G. L.; Busch, D. H. *J. Am. Chem. Soc.* **1983**, *105*, 298. (c) Herron, N.; Zimmer, L. L.; Grzybowski, J. J.; Olszanski, D. J.; Jackels, S. C.; Callahan, R. W.; Cameron, J. H.; Christoph, G. G.; Busch, D. H. *J. Am. Chem. Soc.* **1983**, *105*, 6585. (d) Herron, N.; Dickerson, L.; Busch, D. H. *J. Chem. Soc., Chem. Commun.* **1983**, 884. (e) Herron, N.; Schammel, W. P.; Jackels, S. C.; Grzybowski, J. J.; Zimmer, L. L.; Busch, D. H. *Inorg. Chem.* **1983**, *22*, 1433. (f) Goldsby, K. A.; Beato, B. D.; Busch, D. H. *Inorg. Chem.* **1986**, *25*, 2342.

Scheme II



Scheme III



iron(II). The iron complexes are usually five-coordinate and high spin, with one external axial ligand.⁹ For example, chloride and pyridine cannot enter the cavity. The small ligands O₂ and CO readily bind to the iron within the cavity. A detailed structural analysis has been reported on the cavities of various lacunar cyclidene structures, both with and without included guests.¹⁰

The ligands fall into two groups depending on the substituents R² and R³ (Figure 1), which are either both methyl or respectively benzyl and phenyl. In each group, the three derivatives differ in

- (10) Alcock, N. W.; Lin, W.-K.; Cairns, C.; Pike, G. A.; Busch, D. H. *J. Am. Chem. Soc.* **1989**, *111*, 6630.

Table I. Data Collection and Refinement Details for X-ray Structural Determination of the Nickel(II) Complex [DMNiDM(Me₂Me₂Mxyl[16]cyclidene)](PF₆)₂

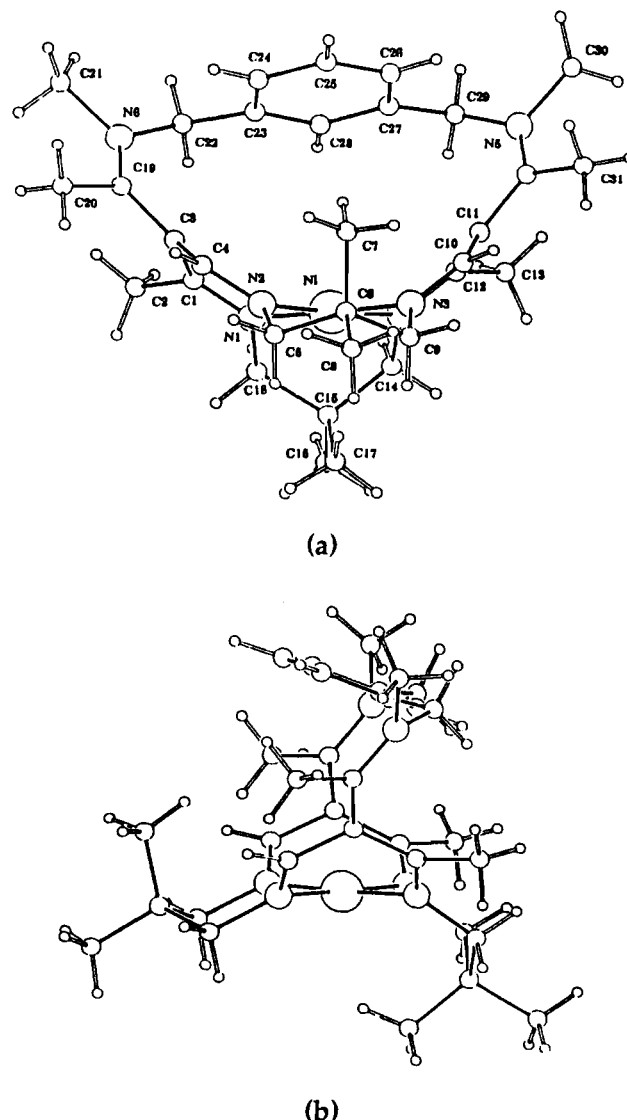
empirical formula	NiC ₃₂ H ₄₈ N ₆ P ₂ F ₁₂
fw	865.412
cryst system	monoclinic
space group	<i>P</i> 2 ₁ / <i>c</i>
<i>a</i> , Å	13.541 (4)
<i>b</i> , Å	15.408 (5)
<i>c</i> , Å	20.471 (7)
β , deg	106.10
<i>V</i> , Å ³	4103 (2)
<i>Z</i>	4
density(calc), g/cm ³	1.41
μ (Mo K α), cm ⁻¹	6.33
diffractometer	Syntex P2 ₁
no. of individual reflns	5240
no. of reflns with <i>I</i> / σ (<i>I</i>) \geq 2.0	3302
cell dimens, mm	0.176 \times 0.481 \times 0.915
<i>R</i> , <i>R</i> _w	0.083, 0.091

the location or number of *gem*-dimethyl groups. We assign the abbreviation DMNi or [DMNi(R³R²[16]cyclidene)]²⁺ to the species having only one such group and with that group on the left-hand side as drawn in Figure 1. For this species, the *gem*-dimethyl group is on the more open side of the cavity. NiDM or [NiDM(R³R²[16]cyclidene)]²⁺ then represents the case where the *gem*-dimethyl group is beneath the bridging group and closest to the methyl substituents on the parent cyclidene macrocycle. Further, DMNiDM or [DMNiDM(R³R²[16]cyclidene)]²⁺ represents the bis(*gem*-dimethyl)-substituted complex.

The synthetic design for placing *gem*-dimethyl groups on the cyclidene macrocycle is outlined in Scheme I. 1,3-Diamino-2,2-dimethylpropane replaces 1,3-diaminopropane in either the initial condensation to form the substituted linear tetradentate complex (NiLTD, 1), the final ring closing step to form the Jäger complexes (2), or both.¹¹ The most challenging step is the final ring closure, using the substituted Jäger complex. The low yields (20–30%) require close adherence to the procedures given. Tables S1 and S2 in the supplementary material provide infrared and NMR data useful for quality control during synthesis. The substitution of a phenyl group at the R³ position used published methods¹³ (Scheme II). The dark green color of the deacylated, deprotonated tetramethyl complex 4b is unusual; purple is the common color. Scheme III follows published procedures,¹³ but the yields for *gem*-dimethyl-substituted complexes were higher than those for the analogous unsubstituted complexes and the new complexes are more easily crystallized.

The new ligand salts were isolated by bubbling HBr gas through a methanolic slurry of the appropriate complex, evaporating the solvent from the resulting bright green solutions, and metathesizing with hexafluorophosphate. HCl gas was inadequate although it has been used routinely in related studies.^{8,9}

X-ray Crystal Structure of [DMNiDM(Me₂Me₂[16]cyclidene)](PF₆)₂ Complex 8c. Figure 2 shows two views of the cationic complex, and Table II lists selected bond distances and angles. The *gem*-dimethyl pairs adopt very different positions in relation to the cavity, and they are controlled by the characteristic boat/chair conformations of the saturated NiN₂C₃ chelate rings. The chelate ring having substituents Y (C16 and C17, Figure 2) is on the same side of the molecule as the methyl groups on the unsaturated chelate rings (C2 and C13, Figure 2); this saturated chelate ring has a boat conformation, as is always observed in

**Figure 2.** ORTEP drawings of [DMNiDM(Me₂Me₂Mxyl[16]cyclidene)](PF₆)₂: (a) view showing atomic numbering scheme; (b) view of same molecule rotated 90°.**Table II.** Selected Bond Lengths (Å) and Angles (deg) for [DMNiDM(Me₂Me₂Mxyl[16]cyclidene)](PF₆)₂

Bond Lengths			
Ni–N(1)	1.902 (6)	C(1)–C(3)	1.445 (12)
Ni–N(2)	1.864 (8)	C(3)–C(4)	1.407 (11)
Ni–N(3)	1.884 (6)	C(3)–C(19)	1.414 (12)
Ni–N(4)	1.900 (8)	C(10)–C(11)	1.438 (13)
N(1)–C(1)	1.266 (10)	C(11)–C(12)	1.436 (11)
N(1)–C(18)	1.477 (10)	C(11)–C(32)	1.434 (13)
N(2)–C(4)	1.304 (11)	C(19)–N(6)	1.306 (13)
N(2)–C(5)	1.484 (11)	C(32)–N(5)	1.301 (13)
N(3)–C(9)	1.476 (11)	N(5)–C(29)	1.445 (11)
N(3)–C(10)	1.267 (12)	N(5)–C(30)	1.477 (16)
N(4)–C(12)	1.307 (12)	N(6)–C(22)	1.485 (13)
N(4)–C(14)	1.478 (11)	N(6)–C(22)	1.462 (14)
Bond Angles			
N(1)–Ni–N(2)	88.4 (3)	C(1)–C(3)–C(4)	117.7 (7)
N(1)–Ni–N(4)	91.1 (3)	C(4)–N(2)–Ni	121.2 (6)
N(2)–Ni–N(3)	92.6 (3)	Ni–N(3)–C(10)	121.6 (6)
N(3)–Ni–N(4)	87.8 (3)	N(3)–C(10)–C(11)	125.0 (7)
Ni–N(1)–C(1)	124.3 (5)	C(10)–C(11)–C(12)	116.3 (8)
N(1)–C(1)–C(3)	121.1 (7)	C(11)–C(12)–N(4)	122.0 (8)

(11) (a) Jäger, E. *Z. Anorg. Allg. Chem.* **1966**, *346*, 76. (b) Jäger, E. *Z. Chem.* **1968**, *8*, 30. (c) Jäger, E. *Z. Chem.* **1968**, *8*, 392.

(12) Korybut-Daszkiewicz, B.; Kojima, M.; Cameron, J. H.; Herron, N.; Chavan, M. Y.; Jircitano, A. J.; Coltrain, B. K.; Neer, G. L.; Alcock, N. W.; Busch, D. H. *Inorg. Chem.* **1984**, *23*, 903.

(13) (a) Busch, D. H.; Olszanski, D. J.; Stevens, J. C.; Schammel, W. P.; Kojima, M.; Herron, N.; Zimmer, L. L.; Holter, K. A.; Mocak, J. J. *Am. Chem. Soc.* **1981**, *103*, 1472. (b) Busch, D. H.; Jackels, S. C.; Callahan, R. W.; Grzybowski, J. J.; Zimmer, L. L.; Kojima, M.; Olszanski, D. J.; Schammel, W. P.; Stevens, J. C.; Holter, K. A.; Mocak, J. *Inorg. Chem.* **1981**, *20*, 2834.

cyclidene complexes having no axial ligands, although it assumes a chair conformation when an axial ligand is present.¹⁰ The steric demands of the *gem*-dimethyl substituents labeled Y must greatly enhance this structural preference, and because of the interde-

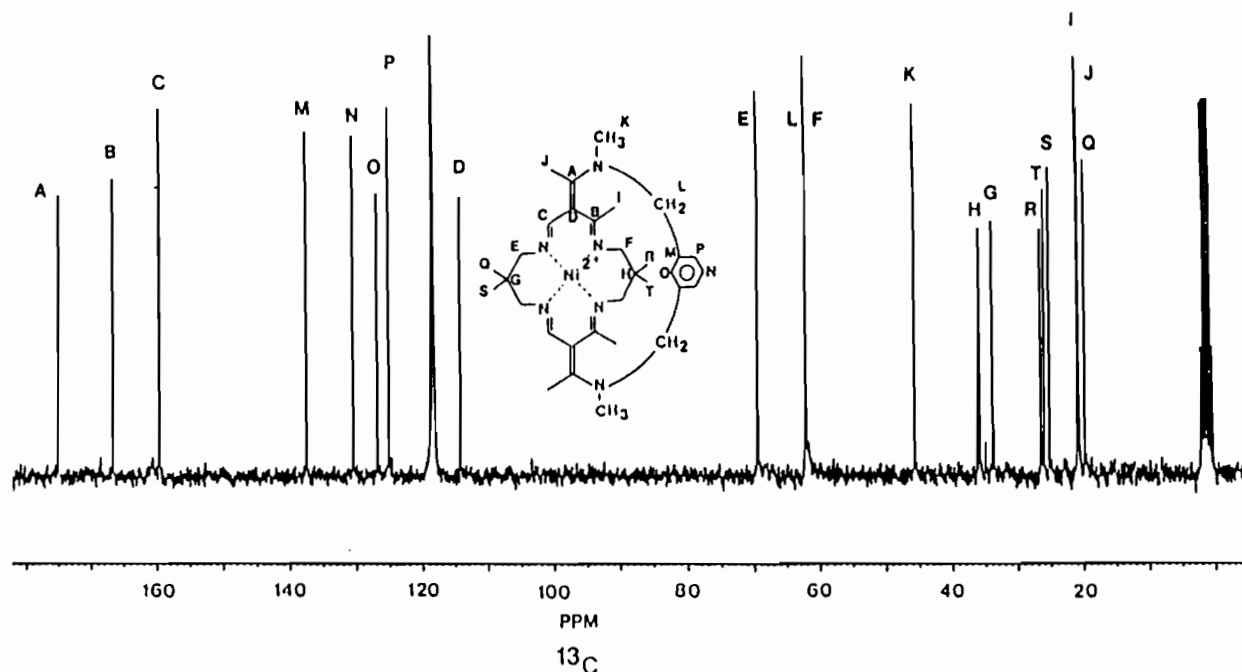


Figure 3. Assigned ^{13}C NMR spectrum of $[\text{DMNiDM}[\text{Me}_2\text{Me}_2\text{Mxyl}[16]\text{cyclidene}]](\text{PF}_6)_2$ in CD_3CN .

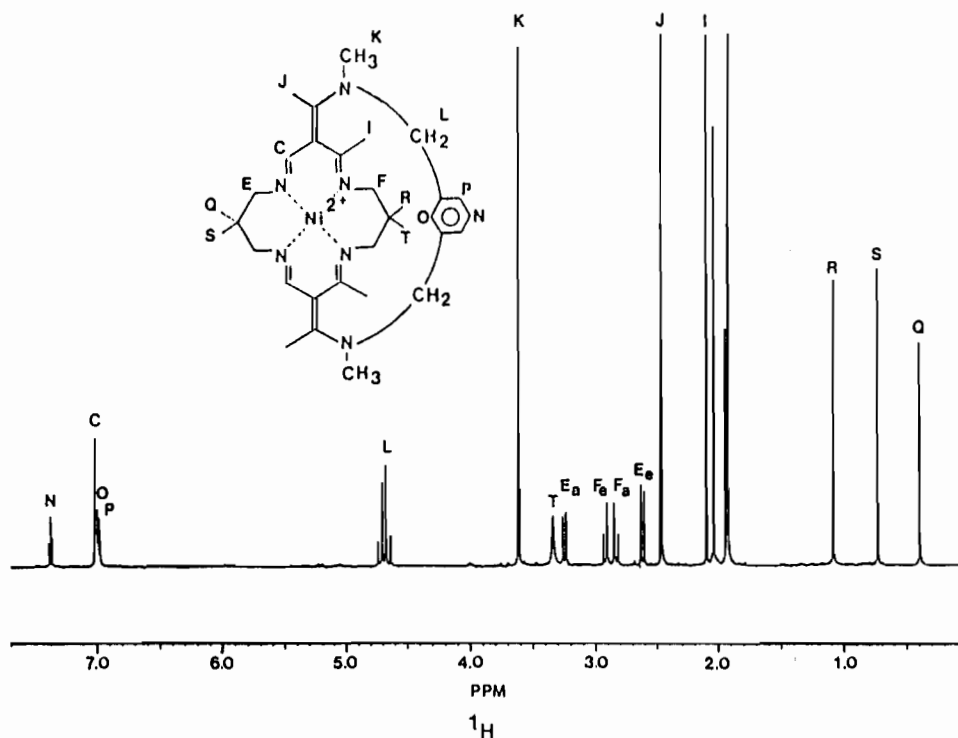


Figure 4. Assigned ^1H NMR spectrum of $[\text{DMNiDM}[\text{Me}_2\text{Me}_2\text{Mxyl}[16]\text{cyclidene}]](\text{PF}_6)_2$ in CD_3CN .

pendence of the conformation of this saturated chelate ring and the binding of ligands in the exterior axial site, the presence of the *gem*-dimethyl group should affect axial ligand binding. The other saturated chelate ring shows a great tendency to assume the chair conformation,¹⁰ but a boat form can exist.¹⁴ Figure 2 strongly suggests that with two *gem*-dimethyl pairs of methyl groups, the boat/boat conformation would be unlikely. Not only does the methyl group having C17 provide a formidable steric hindrance to a potential axial ligand but its near hydrogen atom is only about 2.4 Å from the nickel ($\text{Ni}-\text{C} = 3.031$ Å), a value reminiscent of "agostic" hydrogens.¹⁵ The positioning of the other

gem-dimethyl group, in its characteristic chair conformation, has implications with respect to dioxygen binding. A methyl group, C7, fills a major portion of the opening of the lacuna. In other respects, the structure of **8c** is typical of a *lid-off m*-xylylene complex.^{9c,12} The width of the lacuna from N6 to N5 is 7.32 Å, the height at the front of the cavity (Ni to C25) is 4.78 Å, and that at the back of the cavity (Ni to C28) is 3.97 Å. The corresponding values for the analogous Fe(II) complex (having no *gem*-dimethyl groups and with an axial Cl ligand)^{9c} and the phenyl, *N*-benzyl-substituted Ni complex¹² (also without the *gem*-dimethyl groups) are width 7.34 and 7.27 Å, front height 4.96 and 5.37 Å, and back height 3.57 and 3.74 Å, respectively. Substitution of *gem*-dimethyl groups has resulted in a slight tilting of the bridging benzene ring, so that the front of the cavity is lower and the back higher, but the width is unchanged.

(14) Meade, T. J.; Alcock, N. W.; Busch, D. H. *Inorg. Chem.* 1990, 29, 3766.

(15) Brookhart, M.; Green, M. L. H. *J. Organomet. Chem.* 1983, 250, 395.

NMR Spectra and Solution Structure. The complete assignment of the ^{13}C and ^1H NMR spectra (Figures 3 and 4) of the *gem*-dimethyl-related cyclidene complexes (**8a–c**) was made possible by detailed analysis of 2-dimensional NMR spectra, following earlier studies on a number of unsubstituted cyclidenes.¹⁶ Initial assignments of the ^{13}C spectrum were made from the distortionless enhancement through polarization transfer (DEPT) spectrum. Assignments for carbons A, B, C, D, I, and J (identified in Figure 3) had been made previously by using ^{13}C -labeling techniques¹⁷ and are confirmed by the DEPT experiment. In addition, the amine methyl group K and the quaternary phenyl carbon M could be assigned unambiguously. At this point it can be seen that the *gem*-dimethyl carbons are found in the 20–30 ppm region, with three of the resonances grouped together around 25 ppm and the other shifted upfield at 19.8 ppm. Complete assignment of the methyl resonances provides an explanation for this curious pattern, as discussed later.

The ^1H NMR spectrum of **8c** was assigned from 2-dimensional spectra with (a) a heteronuclear correlated shift spectrum (assigning protons attached to C, I, J, K, and N), and (b) a NOESY experiment indicating through-space proton–proton interactions.¹⁸ The axial and equatorial protons of F cannot be unambiguously identified in this way but were assigned by noting that the F carbon is a member of a saturated six-membered ring and that equatorial protons are generally shifted farther downfield in cyclohexane rings.¹⁶ Table S3 in the supplementary material presents the chemical shift data for this complex and the complexes containing single *gem*-dimethyl pairs, [DMNi{Me₂Me₂Mxyl[16]cyclidene}](PF₆)₂ (**8a**) and [NiDM{Me₂Me₂Mxyl[16]cyclidene}](PF₆)₂ (**8b**).

For [DMNiDM{Me₂Me₂Mxyl[16]cyclidene}](PF₆)₂, the NMR data indicate that its solution structure contains many features of the solid-state structure. The methyl group T (C17) experiences a deshielding effect from the nickel metal center, as a result of its close proximity, and a similar effect is seen for the axial methylene proton H_a in [DMNi{Me₂Me₂Mxyl[16]cyclidene}](PF₆)₂. Such a deshielding influence has been observed in other nickel complexes where vicinal groups interact with the nickel center.¹⁹ The dipolar coupling between the protons of C and Q necessitates the overall saddle shape of the molecule and the chair and boat conformations of the saturated chelate rings. The presence of the permanent void between the metal center and the bridging moiety accounts for the interaction between the benzylic protons L and those of the methyl group I.

Synthesis and Characterization of Fe(II) Complexes. The Fe(II) complexes (**9a–f**) were synthesized under oxygen-free conditions in acetonitrile by using Fe^{II}(py)₂Cl₂ as the source of iron and triethylamine to deprotonate the ligand salt. The resulting paramagnetic complexes were readily soluble in acetonitrile and only slightly soluble in ethanol and were generally red in color, although the complexes with R³ = phenyl were a brownish red. Their infrared spectra are qualitatively the same as those of the parent Ni(II) complexes, but the assessment of the purity of the iron(II) complexes is mainly dependent on elemental analysis. The high sensitivity of these complexes to atmospheric oxidation limits the precision of analytical values, and the variation between observed and expected percentages sometimes exceeded 0.5%. It can reasonably be assumed that the cyclidene ligands are intact, but the coordination environments of the iron centers are less certain. The analytical results suggest that the mono(*gem*-dimethyl) complex [DMFe] is isolated as a [Cl](PF₆) complex, presumably with coordinated chloride, but that the [FeDM] and [DMFeDM] complexes were obtained as [PF₆]₂ salts.

In view of the limitations just described, attempts were made to form the diamagnetic CO adducts of the three complexes: DMFe, FeDM, and DMFeDM (Figure 5). This technique was

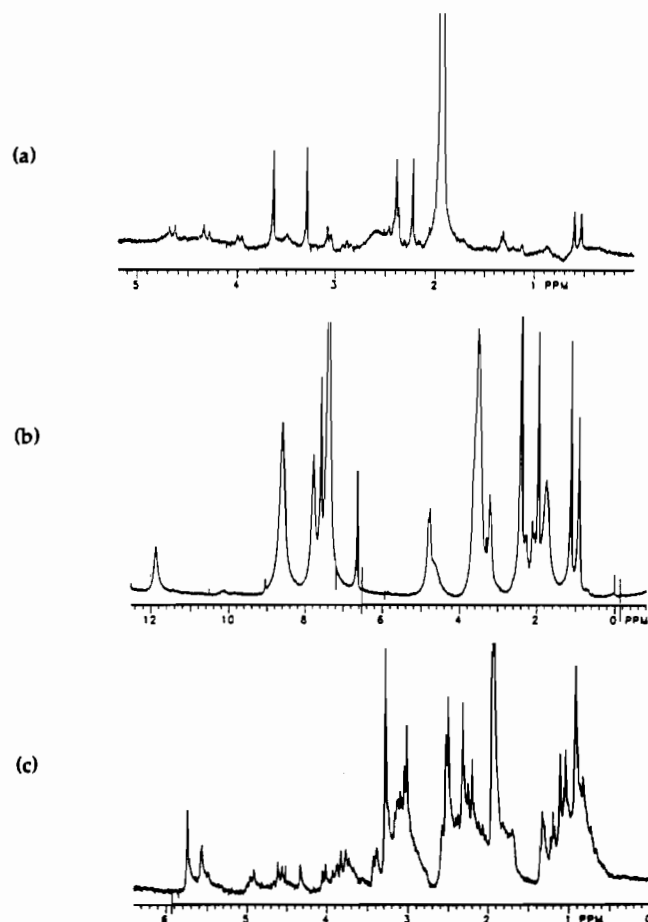


Figure 5. ^1H NMR spectra of iron(II) complexes in CD₃CN/D₂O/pyridine following introduction of CO gas: (a) [DMFe{Me₂Me₂Mxyl[16]cyclidene}Cl](PF₆); (b) [FeDM{Me₂Me₂Mxyl[16]cyclidene}](PF₆)₂; (c) [DMFeDM{Me₂Me₂Mxyl[16]cyclidene}](PF₆)₂.

Table III. Electrochemical Data^a for Ni(II) and Fe(II) Complexes in 0.1 M TBAT/CH₃CN

complex	$E_{1/2}^b$, V	ΔE_p^c , mV
[DMNi{Me ₂ Me ₂ Mxyl[16]cyclidene}Cl](PF ₆)	0.80	80
[NiDM{Me ₂ Me ₂ Mxyl[16]cyclidene}Cl](PF ₆)	0.82	90
[DMNiDM{Me ₂ Me ₂ Mxyl[16]cyclidene}Cl](PF ₆)	0.82	90
[Ni{Me ₂ Me ₂ Mxyl[16]cyclidene}Cl](PF ₆) ^d	0.78	90
[DMNi{Ph ₂ Bz ₂ Mxyl[16]cyclidene}Cl](PF ₆)	1.02	75
[NiDM{Ph ₂ Bz ₂ Mxyl[16]cyclidene}Cl](PF ₆)	1.02	100
[DMNiDM{Ph ₂ Bz ₂ Mxyl[16]cyclidene}Cl](PF ₆)	1.02	90
[Ni{Ph ₂ Bz ₂ Mxyl[16]cyclidene}Cl](PF ₆) ^d	0.99	80
[DMFe{Ph ₂ Bz ₂ Mxyl[16]cyclidene}Cl](PF ₆) ^e + xs LiCl	-0.19 ^f	65
[FeDM{Ph ₂ Bz ₂ Mxyl[16]cyclidene}Cl](PF ₆) ^e + xs LiCl	-0.21	80
[DMFeDM{Ph ₂ Bz ₂ Mxyl[16]cyclidene}Cl](PF ₆) ^e + xs LiCl	-0.26 ^f	70
[DMFeDM{Ph ₂ Bz ₂ Mxyl[16]cyclidene}Cl](PF ₆) ^e	-0.26	75
[DMFeDM{Ph ₂ Bz ₂ Mxyl[16]cyclidene}Cl](PF ₆) ^e	-0.22 ^g	115
[Fe{Ph ₂ Bz ₂ Mxyl[16]cyclidene}Cl](PF ₆) ^{e,h} + xs LiCl	-0.22 ^f	60
	-0.22	75

^a Measured at platinum disk electrode. ^b Vs Ag/AgNO₃. ^c $\Delta E_p = (E_p^c - E_p^a)$. ^d Taken from ref 14. ^e Measured at silver wire electrode. ^f Vs ferrocene (+/0). ^g Value less reliable; attempts to reproduce this value suggested sample had deteriorated. ^h Taken from ref 8c.

used by Zimmer²⁰ with a variety of iron(II) cyclidene complexes to obtain diamagnetic species that were subsequently characterized by NMR spectroscopy. The ^1H NMR experiment was successful in producing a sharp NMR spectrum only with FeDM, and for that case, the expected ligand was indeed found to be present. The presence of many bands over a wide range of chemical shifts indicated that the solutions of the other two complexes contained

(16) Meade, T. J.; Fendrick, C. M.; Padolik, P. A.; Cottress, C. E.; Busch, D. H. *Inorg. Chem.* **1978**, *26*, 4252.

(17) Takeuchi, K. J.; Busch, D. H. *J. Am. Chem. Soc.* **1983**, *105*, 6812.

(18) Padolik, P. A. Ph.D. Thesis, The Ohio State University, 1989.

(19) Warner, L. G.; Rose, N. J.; Busch, D. H. *J. Am. Chem. Soc.* **1967**, *89*, 703.

(20) Zimmer, L. L. Ph.D. Thesis, The Ohio State University, 1979.

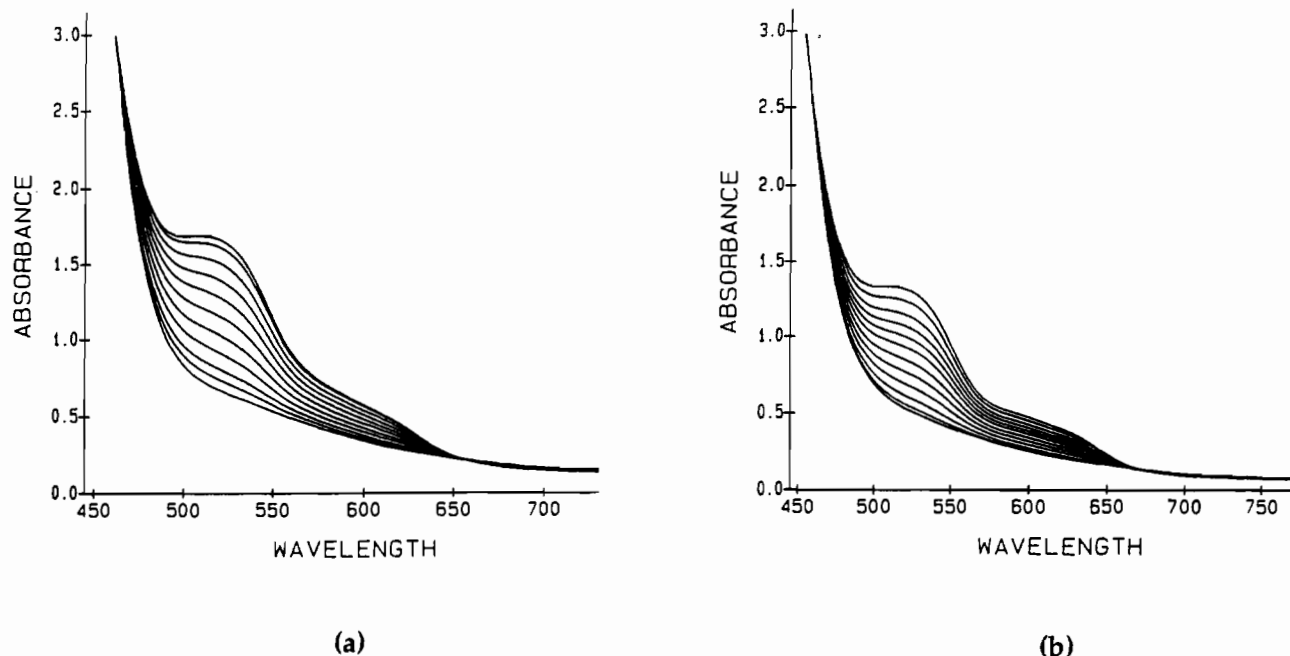


Figure 6. (a) Visible spectra upon oxygenation of $[\text{DMFe}\{\text{Ph}_2\text{Bz}_2\text{Mxyl}\}[16]\text{cyclidene}\text{Cl}](\text{PF}_6)$ at $-40.0\text{ }^\circ\text{C}$ in 3:1:1 acetone/pyridine/water. (b) Visible spectra upon oxygenation of $[\text{FeDM}\{\text{Ph}_2\text{Bz}_2\text{Mxyl}\}[16]\text{cyclidene}\text{Cl}](\text{PF}_6)$ at $-20.0\text{ }^\circ\text{C}$ in 3:1:1 acetone/pyridine/water.

Table IV. Dioxygen Binding Equilibrium Constants^a for the Iron Complexes $[\text{XFeY}\{\text{Ph}_2\text{Bz}_2\text{Mxyl}\}[16]\text{cyclidene}\text{Cl}](\text{PF}_6)$

<i>T</i> , °C	[DMFe]	[FeDM]	[Fe]
-45.0	0.016 (2)		
-42.2	0.013 (1)		
-40.0	0.011 (1)		
-35.0	0.0061 (3)		0.35 ^b
-30.0	0.003 (1)		0.16 ^b
-24.5		0.36 (1)	0.069 ^b
-20.0		0.21 (1)	0.036 ^b
-15.0		0.101 (2)	
-10.0		0.067 (2)	0.0091 (2) ^c
0.0		0.018 (2)	0.0025 (4) ^c

^a Measured in 3:1:1 acetone/pyridine/water; units of Torr⁻¹.

^b Values interpolated from data in ref 8c. ^c Actual data from ref 8c.

much paramagnetic material. Clearly the formation of the CO adduct was incomplete with DMFe and DMFeDM.

Electrochemical Behavior. Cyclic voltammetric studies were carried out on all of the complexes $[\text{XMY}\{\text{Me}_2\text{Me}_2\text{Mxyl}\}[16]\text{cyclidene}\text{Cl}](\text{PF}_6)_2$ and $[\text{XMY}\{\text{Ph}_2\text{Bz}_2\text{Mxyl}\}[16]\text{cyclidene}\text{Cl}](\text{PF}_6)_2$, where X, Y = CH₃ or H (8,9a-f), in acetonitrile with 0.1 M tetra-*n*-butylammonium tetrafluoroborate or chloride as the supporting electrolyte. Most of the results are summarized in Table III.

Equilibrium Constants for O₂ Binding. Typical examples of the change in the electronic spectra that occurs upon bubbling increasing partial pressures of dioxygen through the solution of an iron cyclidene complex are shown in Figure 6a,b for the complexes $[\text{DMFe}\{\text{Ph}_2\text{Bz}_2\text{Mxyl}\}[16]\text{cyclidene}\text{Cl}](\text{PF}_6)$, $[\text{DMFe}]$, and $[\text{FeDM}\{\text{Ph}_2\text{Bz}_2\text{Mxyl}\}[16]\text{cyclidene}\text{Cl}](\text{PF}_6)$, $[\text{FeDM}]$, respectively. The addition of dioxygen changes the relatively featureless visible spectrum of the unoxygenated species to that of the dioxygen adduct, which exhibits a peak at 520 nm and a shoulder at 610 nm for $[\text{DMFe}]$ or 630 nm for $[\text{FeDM}]$.

The equilibrium constants for dioxygen binding by the *gem*-dimethyl monosubstituted iron(II) complexes were calculated from the spectroscopic absorbance values at various partial pressures of dioxygen. These data were treated by the method of Stevens²⁰ with a local computer program written by Dr. Naidong Ye.²¹ The K_{O_2} results are listed in Table IV; values for the unsubstituted parent complex are included for comparison purposes.

Discussion

Effects of the *gem*-Dimethyl Group on Coordination Number.

The electrochemical data in Table III show that little or no electron density is placed on the metal by the *gem*-dimethyl group. The $E_{1/2}$ values of the Ni²⁺/³⁺ couples for the two classes of cyclidenes (Me₂Me₂ versus Ph₂Bz₂) differ by about 200 mV, and this can be attributed to electronic effects. In contrast, the *gem*-dimethyl derivatives differ from the corresponding unsubstituted species by only about 30–40 mV, a value that is only slightly greater than the uncertainty in the numbers. The cyclic voltammograms for the metal ion couples are reasonably reversible, and oxidation waves attributed to ligand oxidation occur at potentials that are 200 mV more anodic. The behavior of the Ph₂Bz₂/iron(II) derivatives is completely parallel.

The behavior of the complexes $[\text{XFeY}\{\text{Me}_2\text{Me}_2\text{Mxyl}\}[16]\text{cyclidene}\text{Cl}](\text{PF}_6)_2$ is much more revealing. The complex with one *gem*-dimethyl group on the sterically less demanding side of the molecule (X = Me, Y = H), $[\text{DMFe}\{\text{Me}_2\text{Me}_2\text{Mxyl}\}[16]\text{cyclidene}\text{Cl}](\text{PF}_6)_2$ (9a), exhibits characteristic reversible behavior with $E_{1/2}$ corresponding to the Fe²⁺/³⁺ couple at -0.41 V vs Ag/AgNO₃, a value that is very close to that (0.40 V) for the analogous parent complex.^{9c} However, in marked contrast, when Y = Me, on the opposite side of the molecule in either $[\text{FeDM}\{\text{Me}_2\text{Me}_2\text{Mxyl}\}[16]\text{cyclidene}\text{Cl}](\text{PF}_6)$ (9b) or the bis(*gem*-disubstituted) complex 9c reversible couples are observed at much more anodic potentials, around -0.04 V . The cyclic voltammogram of the $[\text{DMFeDM}]$ complex (Figure 7) shows a smaller reversible wave at -0.25 V , along with the major wave at -0.04 V . Addition of tetra-*n*-butylammonium bromide to the solution caused an increase in the weaker signal, indicating that a small amount of the complex exists with bromide as an axial ligand. This is possible, since bromide ion is present in the ligand salt as a result of the demetalation with HBr.

Proof that chloride is neither the principal axial ligand nor responsible for the smaller wave is seen in Figure 7b. Addition of an excess of tetra-*n*-butylammonium chloride to the iron complex produces a couple at -0.38 V , as expected for the chloro complex. Even under these conditions of excess chloride ion, the wave at -0.04 V remains the dominant signal, indicating that the coordination of the chloride ion is in some way restricted.

The corresponding complex having no *gem*-dimethyl group readily forms an acetonitrile complex in that solvent, and the associated Fe³⁺/Fe²⁺ couple has an $E_{1/2}$ value of -0.12 V .^{9c} Consequently, the wave at -0.04 V is not likely to be due to the

(21) Ye, N. Ph.D. Thesis, The Ohio State University, 1989.

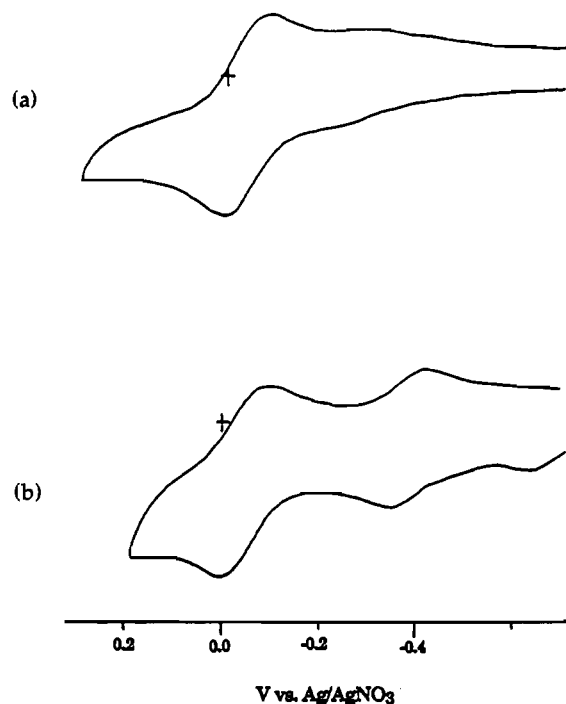


Figure 7. Cyclic voltammograms of $[\text{DMFeDM}(\text{Me}_2\text{Me}_2\text{Mxyl}[16]\text{cyclidene})](\text{PF}_6)_2$: (a) sample in $\text{TBAT}/\text{CH}_3\text{CN}$; (b) same solution as (a) plus excess of tetra-*N*-butylammonium chloride.

complex containing acetonitrile as the axial base. The relatively more anodic potential of this feature suggests the possibility that no ligand is bound at the axial site; i.e., the complex exists to a large degree as a *four-coordinate* species. This is consistent with the expectation of the chair conformation for the chelate ring positioned beneath the bridging group and the great repulsion predicted between the *gem*-dimethyl group and the axial ligand.

To test the validity of the inferred four-coordinate structure, Evan's moment experiments were run on the three *m*-xylylene-bridged iron(II) complexes XFeY . A four-coordinate iron(II) complex would be expected to exist in the intermediate spin state ($I = 2$), and the spin-only magnetic moment for such a species would be $2.82 \mu_B$. The complex $[\text{DMFe}(\text{Me}_2\text{Me}_2\text{Mxyl}[16]\text{cyclidene})\text{Cl}](\text{PF}_6)_2$ gave a magnetic moment of $5.15 \mu_B$, which is within the acceptable range for high-spin iron(II) and is typical of the five-coordinate cyclidene complexes.^{9c} However, the complexes $[\text{FeDM}(\text{Me}_2\text{Me}_2\text{Mxyl}[16]\text{cyclidene})](\text{PF}_6)_2$ and $[\text{DMFeDM}(\text{Me}_2\text{Me}_2\text{Mxyl}[16]\text{cyclidene})](\text{PF}_6)_2$ were found to have considerably lower magnetic moments ($\mu = 3.9$ and $3.5 \mu_B$, respectively), providing evidence for the occurrence of spin pairing and in agreement with the presumed partial existence of the complexes in the four-coordinate state. Since the electrochemical results clearly indicate a mixture of four- and five-coordinate species, the agreement can be considered conclusive.

Dioxygen Binding. The dioxygen binding abilities of the *gem*-dimethyl-substituted iron(II) complexes were studied by using the cyclidene system where the bridging group R^1 is *m*-xylylene, R^2 is benzyl, and R^3 is phenyl (labeled for convenience $[\text{DMFe}]$, $[\text{FeDM}]$, and $[\text{DMFeDM}]$). Because the cavity in the complexes is unsymmetrical, the complexes with $\text{X} = \text{Me}$ can be described as substituted at the *front* of the cavity (its wider opening), while those with $\text{Y} = \text{Me}$ are substituted at its back. This set of substituents was chosen because the parent complex $[\text{Fe}\{\text{Ph}_2\text{Bz}_2\text{Mxyl}[16]\text{cyclidene}\}\text{Cl}](\text{PF}_6)$ (labeled $[\text{Fe}]$) was found to exhibit measurable values for the dioxygen binding equilibrium constant, K_{O_2} , while undergoing minimal autoxidation at readily accessible temperatures.⁹ Studies of dioxygen binding ability were performed in 3:1:1 by volume acetone/pyridine/water. K_{O_2} values for the iron cyclidenes have typically been obtained in this rather unusual solvent mixture,⁹ in which the acetone solubilizes the cyclidene complex and allows for low-temperature study without freezing; water labilizes the tightly bound axial chloride ligand,

Table V. Thermodynamic Parameters for Dioxygen Binding

complex	ΔH , kcal/mol	ΔS , cal/(K·mol)
$[\text{DMFe}\{\text{Ph}_2\text{Bz}_2\text{Mxyl}[16]\text{cyclidene}\}\text{Cl}](\text{PF}_6)$	-12.1 ± 0.8	-61 ± 3
$[\text{FeDM}\{\text{Ph}_2\text{Bz}_2\text{Mxyl}[16]\text{cyclidene}\}\text{Cl}](\text{PF}_6)$	-16.6 ± 0.5	-69 ± 2
$[\text{Fe}\{\text{Ph}_2\text{Bz}_2\text{Mxyl}[16]\text{cyclidene}\}\text{Cl}](\text{PF}_6)^a$	-17.5 ± 0.4	-76 ± 2

^aReference 8c.

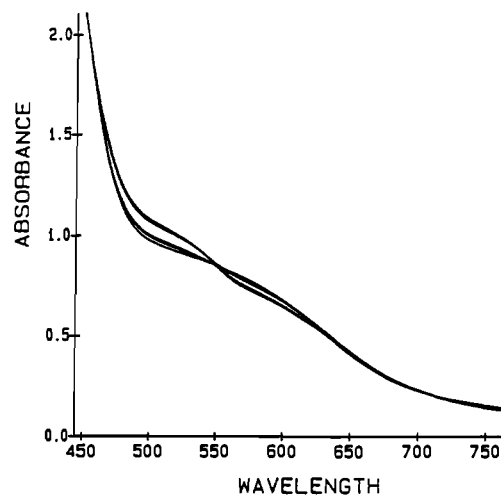


Figure 8. Visible spectra upon oxygenation of $[\text{DMFeDM}\{\text{Ph}_2\text{Bz}_2\text{Mxyl}[16]\text{cyclidene}\}\text{Cl}](\text{PF}_6)$ at -40.0°C in 3:1:1 acetone/pyridine/water.

allowing pyridine to replace the chloride, which, in turn, enhances the ability of the metal center to bind dioxygen.

The equilibrium constant for $[\text{FeDM}]$ (Table IV) is 6–9 times higher than that for the parent complex, which in turn has a higher K_{O_2} value than that for $[\text{DMFe}]$ by a factor of about 50. In fact, the latter $[\text{DMFe}]$ has so low a dioxygen affinity that measurable values for K_{O_2} could only be obtained at temperatures of -30°C and below. Substituting *gem*-dimethyl groups on the cyclidene macrocycle does indeed exert a significant effect on the dioxygen binding ability of the iron(II) complexes.

The axial methyl group on the front (open) side of the lacuna in $[\text{DMFe}]$ interferes with O_2 binding, probably through direct steric repulsion between the methyl group and the bound O_2 . Thus, substitution at this position provides another structural tool for controlling the dioxygen affinities of cyclidene complexes. It should be recalled that the first successful observation of reversible O_2 binding by iron(II) cyclidene complexes depended on drastically reducing the dioxygen affinity so that the O_2 could be removed from the complex under moderate conditions.⁹

The contrary behavior of $[\text{FeDM}]$, in which the *gem*-dimethyl group is adjacent to the back or closed side of the lacuna, also has clear implications. Since the dioxygen affinity is large (greater than that of the parent complex), an effective axial ligand must be present.²² For this to happen, the saturated chelate ring having the *gem*-dimethyl group must have adopted the chair conformation. The fact that the O_2 affinity is enhanced over that of the parent complex suggests that the *cavity is enlarged* by the conformational change that is required in order to accommodate the chair conformation of the bulky chelate ring.

Thermodynamic parameters appear in Table V, where, again, the values for the parent complex are included for comparison. The most striking observation is the ΔH value for $[\text{DMFe}]$. It is apparent that the poor dioxygen binding ability for this complex is associated with this term, since the entropy term, which is approximately equal to the entropy of gaseous dioxygen,^{7c} is less negative than those of the other complexes. Their more negative entropies suggest that additional reordering of the ligand or the

(22) A number of studies show this to be the case, e.g.: Carter, M. J.; Rillema, D. P.; Basolo, F. *J. Am. Chem. Soc.* 1974, 96, 392. See also refs 7 and 8, especially 8f.

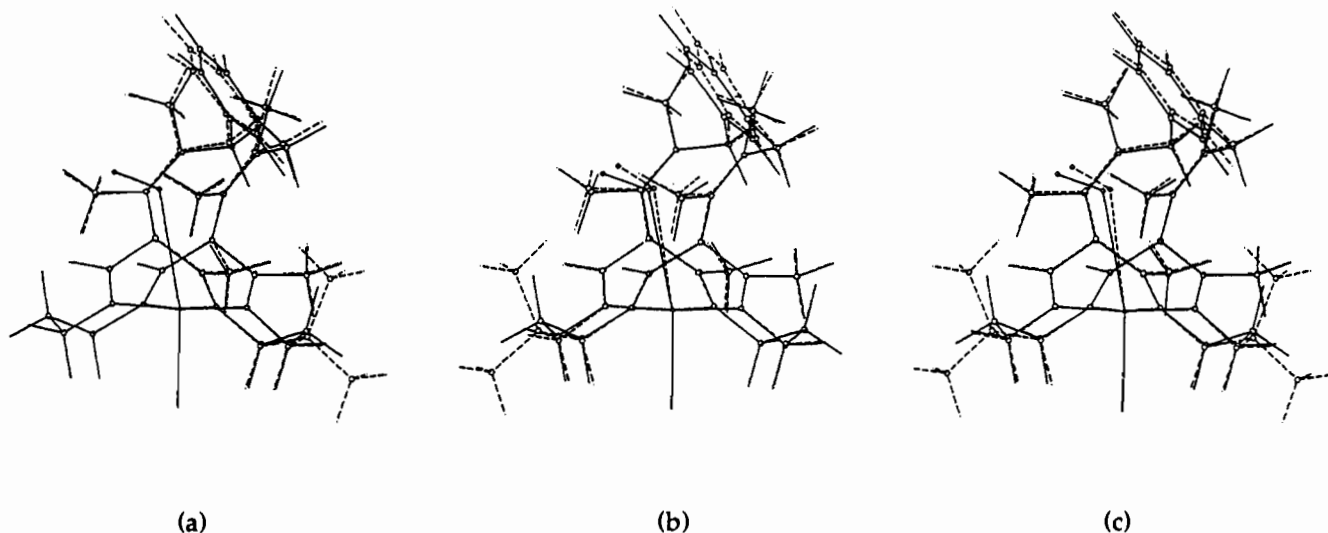


Figure 9. Superimposed structures of dioxo adducts of cobalt cyclidenes: solid line, structure of reference complex $[\text{Co}(\text{Me}_2\text{Me}_2\text{Mxyl}[16]\text{cyclidene})\text{Cl}(\text{O}_2)]^+$; broken line, molecular mechanics generated structure of (a) $[\text{DMCo}(\text{Me}_2\text{Me}_2\text{Mxyl}[16]\text{cyclidene})\text{Cl}(\text{O}_2)]^+$, (b) $[\text{CoDM}(\text{Me}_2\text{Me}_2\text{Mxyl}[16]\text{cyclidene})\text{Cl}(\text{O}_2)]^+$, and (c) $[\text{DMCoDM}(\text{Me}_2\text{Me}_2\text{Mxyl}[16]\text{cyclidene})\text{Cl}(\text{O}_2)]^+$.

solvent must take place on dioxo binding. The parent complex and $[\text{FeDM}]$ exhibit enthalpy values that are the same within experimental error; however, the latter has a less negative entropy, indicating that less reorganization is necessary for this complex.

Placement of the *gem*-dimethyl group on one side of the complex or the other results in a difference in dioxo binding by a factor of approximately 300 but ranging on both sides of the corresponding unsubstituted complex. The result of substitution of these groups simultaneously at *both* positions was therefore not predictable. The result of the K_{O_2} experiment for the complex $[\text{DMFeDM}]$ at -40.0°C in 3:1:1 APW (Figure 8) indicates that this complex displays little or no dioxo binding ability even at this low temperature. The spectral trace prior to oxygenation provides some insight into this surprising result. That spectrum features a broad shoulder at 560 nm, in contrast to the virtually featureless spectra of either singly substituted complex. This spectrum of the bis(*gem*-dimethyl)-disubstituted complex is reminiscent of that of the complex $[\text{Fe}[\text{Me}_2\text{Me}_2\text{Mxyl}[16]\text{cyclidene}]\text{Cl}](\text{PF}_6)$ in acetone, where the axial ligand is the very weak chloride ion.^{9c} Recalling the results of electrochemical and magnetochemical studies in acetonitrile solutions, it is likely that this solution contains a mixture of four-coordinate and five-coordinate iron(II) species. Further, when present, the fifth ligand is chloride. Therefore, for the complex with *gem*-dimethyl groups on both sides, the steric influences compound to confound the O_2 binding process. The absence of an axial ligand or, almost equally, the presence of a very weak axial ligand would produce a greatly reduced dioxo affinity. However, this affinity is further diminished by the direct repulsion between any ligand in the cavity and the axial methyl group at the front of the cavity. This explains the lack of any observable binding of dioxo by the complex $[\text{DMFeDM}]$.

Molecular Modeling. The $E_{1/2}$ values both for the Ni(II) complexes (8a–f) and for the phenyl benzyl substituted Fe(II) complexes (9d–f) show that the marked effects of *gem*-dimethyl substitution are steric in origin. In order to examine these steric interactions in further detail, minimum energy conformations were modeled by molecular mechanics calculations, using a locally modified version of the program MM2/MMP2.²³ These calculations have been validated by their successful application to the binding of O_2 by cyclidene complexes with polymethylene bridges.¹⁰ The results are presented in Figure 9 in the form of comparisons

between the minimized structures including *gem*-dimethyl substituents (dashed lines) and that of a reference structure having no such substituents (solid lines, X-ray structure of $[\text{O}_2\text{Co}[\text{Me}_2\text{Me}_2\text{Mxyl}[16]\text{cyclidene}]\text{Cl}]^+$). These images emphasize the qualitative effects of *gem*-dimethyl substitution, but it should be noted that they relate to complexes all including an axially coordinated atom; they do not confront the issue of hindering the binding of axial ligands. Figure 9a shows the $[\text{CoDM}]$ complex with the *gem*-dimethyl substitution at the back of the cavity. Most of the atoms are unmoved, with only the bridge and other atoms at the top of the structure suffering displacements. The bridge is bent slightly forward by the repulsion of the *gem*-dimethyl group, and the Co–O–O linkage is virtually unaffected. While it remains uncertain why this structural modification enhances the dioxo affinity of the complex, it is clear that the steric repulsions are small. The increased dioxo affinity can be rationalized intuitively by the premise that the interaction between the *gem*-dimethyl group and the bridge must alter the shape of the cavity in such a way that it becomes more accessible for dioxo binding. This is supported in part by the less negative entropy value for this complex compared to the unsubstituted complex, suggesting that $[\text{FeDM}]$ indeed requires less reorganization than $[\text{Fe}]$ to accommodate dioxo.

In contrast, Figure 9b demonstrates that the presence of a *gem*-dimethyl group in front of the cavity has a profound influence on both the shape of the complex and the Co–O–O linkage. The salient feature is the position of the bound dioxo molecule. Repulsion by the axial methyl group pushes the dioxo up and into the cavity, forcing a substantial displacement of the *m*-xylene roof. The significance of this interaction is seen in the displacement of many of the other atoms in the structure as well. Not only is the bridging benzene tilted upward but the saturated portion of the macrocycle containing the *gem*-dimethyl group is pushed down and away, producing a flatter chelate ring conformation. It is evident that this sterically induced deviation from the ideal bonding geometry contributes to the poor dioxo binding ability of this complex.

Figure 9a,b shows that a *gem*-dimethyl group pushes the benzene ring in opposite directions, depending on which side of the lacuna is substituted. Figure 9c shows that the effect of both pairs of substituents $[\text{DMFeDM}]$ is similar to that of a single front-group $[\text{DMFe}]$. As in the $[\text{DMFe}]$ case, the dioxo group is displaced from its reference location. However, steric interference from the methyl group on the back of the cavity prevents the benzene ring from tilting up and away from the Co–O–O linkage. The combination of these two steric effects reduces the dioxo affinity so greatly that dioxo binding can hardly be detected experimentally.

(23) (a) Allinger, N.; Yuh, Y. MM2/MMP2, QCPE Program No. 395. Indiana University, 1980. (b) Allinger, N.; Sprague, J. *J. Am. Chem. Soc.* **1972**, *95*, 3893. Allinger, N. *J. Am. Chem. Soc.* **1977**, *99*, 8129.
(24) Perrins, D. D.; Armarego, L. F.; Perrins, D. R. *Purification of Laboratory Chemicals*; Pergamon Press: Oxford, England, 1980.

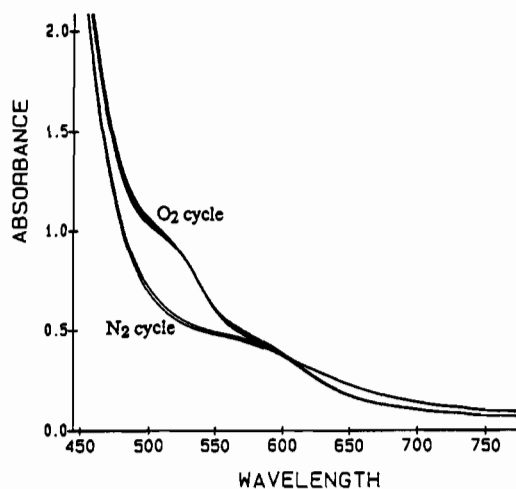


Figure 10. Visible spectra of $[\text{FeDM}(\text{Me}_2\text{Me}_2\text{Mxyl}[16]\text{cyclidene})\text{Cl}](\text{PF}_6)_2$ in 4:1 acetonitrile/*N*-methylimidazole following several successive N_2/O_2 purge cycles at room temperature.

Autoxidation Studies. Previous work with the unsubstituted complex $[\text{Fe}(\text{Ph}_2\text{Bz}_2\text{Mxyl}[16]\text{cyclidene})\text{Cl}](\text{PF}_6)_2$ has shown this complex to be remarkably resistant toward autoxidation, even at room temperature. Simple experiments indicate that the *gem*-dimethyl derivatives exhibit similar stability. A reversibility study was performed on the complex $[\text{FeDM}]$ in a 4:1 acetonitrile/*N*-methylimidazole solution at room temperature. The complex was subjected to alternating cycles of exposure to N_2 and O_2 ; the gas was bubbled through the solution for 300 s with 30-min equilibration periods between bubbling. Figure 10 shows that the complex binds dioxygen with virtually no decomposition over a series of oxygenation/deoxygenation cycles at room temperature. In protic solvents, the autoxidation rate is conveniently measurable. However, the process is complicated and meaningful comparisons cannot be made prior to detailed kinetic studies.

Experimental Section

General Procedures. All syntheses and manipulations of iron(II) complexes were performed under an atmosphere of dry, oxygen-free (<2 ppm) nitrogen in a Vacuum Atmospheres glovebox. Solvents used in the synthesis and study of all Fe(II) complexes were dried by conventional methods,⁹ and care was taken to remove O_2 . Elemental analyses were by Galbraith Laboratories, Inc., or the Department of Molecular Biology, The University of Kansas.

Physical Measurements. Infrared spectra were obtained with a Perkin-Elmer model 283B infrared spectrophotometer using KBr pellets for air-stable samples and Nujol mulls (glovebox) for all air-sensitive complexes. Proton and ^{13}C NMR spectra were obtained by using a Bruker WP200, Bruker AM500, or Varian XT-300 spectrometer, with deuterated solvents as internal reference vs TMS. Magnetic susceptibility measurements were performed on the Bruker WP200 instrument by the Evans method²⁵ using a Wilmad coaxial capillary tube and were corrected for diamagnetic contributions from the ligand by using Pascal's constants.²⁶ Electrochemical data were obtained by Dr. Ken Goldsby and Dr. Richard Warburton using a Princeton Applied Research Corp. Model 173 potentiostat/galvanostat equipped with a Model 175 linear programmer and a Model 179 digital coulometer. Current versus potential curves were measured on a Houston Instruments Model 200 XY recorder. Cyclic voltammograms were run anaerobically in acetonitrile solutions containing 0.1 M tetrabutylammonium tetrafluoroborate (TBAT) by using a platinum disk working electrode, referenced vs a 0.1 M $\text{Ag}/\text{AgNO}_3/\text{CH}_3\text{CN}$ electrode or vs Ag wire with ferrocene as an internal reference. Half-wave potentials were measured as the average of the anodic and cathodic peak potentials at a scan rate of 100 mV/s.

Electronic spectra were obtained by using a Varian 2300 UV/vis spectrophotometer. Equilibration of iron(II) complexes with dioxygen

at various partial pressures was achieved in a thermostated cell using a mass flowmeter/mass flow controller system (Tylan Corp., Carson, CA) to accurately mix dioxygen and dinitrogen standards. The gas mixture was first saturated with solvent vapor in a simple bubbler cell.

Synthesis of Cyclidene Precursor Compound. 3,11-Diacetyl-2,12-dihydroxy-7,7-dimethyl-5,9-diaza-trideca-1,3,9,11-tetraene, $\text{DM}[16]\text{LTD}$. This compound was synthesized according to the procedure of Riley,²⁷ using 2,2-dimethyl-1,3-diaminopropane (DMDAP). Assistance in this preparation was provided by Ms. Elizabeth Drotleff. Yield: 115 g (62%).

Synthesis of Unbridged Nickel(II) Complexes. (3,11-Diacetyl-2,12-dihydroxy-7,7-dimethyl-5,9-diaza-trideca-1,3,9,11-tetraenoato- $\kappa^2\text{N}\kappa^2\text{O}$)-nickel(II), $\text{DMNi}[16]\text{LTD}$. This compound was synthesized according to the procedure of Riley,²⁷ using nickel acetate ($\text{Ni}(\text{OAc})_2 \cdot 4\text{H}_2\text{O}$, 85 g, 0.34 mol) and $\text{DM}[16]\text{LTD}$ (110 g, 0.34 mol). Yield: 96 g (74%). Anal. Calc for $\text{C}_{17}\text{H}_{24}\text{N}_2\text{O}_4\text{Ni}$: C, 53.86; H, 6.38; N, 7.39. Found: C, 53.68; H, 6.34; N, 7.56.

(3,11-Diacetyl-2,7,12-tetramethyl-1,5,9,13-tetraazacyclohexadeca-1,3,9,11-tetraenoato- $\kappa^4\text{N}$)-nickel(II), $\text{DMNi}(\text{Ac}_2\text{Me}_2[16]\text{tetraenoatoN}_4)$. $\text{DMNi}[16]\text{LTD}$ (46 g, 0.12 mol) was added to 130 mL of freshly distilled 1,3-diaminopropane (from KOH). The slurry was brought to reflux. After approximately 10–15 min, an orange solid precipitated. The solution was cooled, 50 mL of water was added, and the precipitate was collected by filtration. The orange solid was washed with copious amounts of water and dried in vacuo at room temperature. Yield: 78%, based on starting complex.

(3,11-Diacetyl-2,12,15,15-tetramethyl-1,5,9,13-tetraazacyclohexadeca-1,3,9,11-tetraenoato- $\kappa^4\text{N}$)-nickel(II), $\text{NiDM}(\text{Ac}_2\text{Me}_2[16]\text{tetraenoatoN}_4)$. To a 100-mL round-bottom flask was added 10 g of $\text{Ni}[16]\text{LTD}$ (0.028 mol)¹² and 30 mL of DMDAP. The purple solution was heated to boiling, and 10 mL of toluene was added. The solution was heated to reflux for 1 h, and the solvent was distilled off under reduced pressure until 30 mL had been collected and the reaction was a thick reddish orange mixture. Addition of 80 mL of ice water resulted in the formation of a brown solid. The solid was collected, dried in air, and redissolved in CHCl_3 . The solution was then passed through a neutral alumina column with CHCl_3 as the eluent, collecting the fastest moving orange band. The solvent volume was reduced, and precipitation was induced by the addition of diethyl ether, giving an orange powder. Yield: 1.5 g (13%). Anal. Calc for $\text{C}_{20}\text{H}_{30}\text{N}_4\text{O}_2\text{Ni}$: C, 57.58; H, 7.25; N, 13.43. Found: C, 57.44; H, 7.70; N, 13.48.

(3,11-Diacetyl-2,7,12,15,15-hexamethyl-1,5,9,13-tetraazacyclohexadeca-1,3,9,11-tetraenoato- $\kappa^4\text{N}$)-nickel(II), $\text{DMNiDM}(\text{Ac}_2\text{Me}_2[16]\text{tetraenoatoN}_4)$. Freshly distilled DMDAP (30 mL) and 30 g of $\text{DMNi}[16]\text{LTD}$ (0.079 mol) were placed in a 500-mL round-bottom flask and heated until a lavender solid was obtained. The solid was then slurried in 200 mL of toluene, and the mixture was heated to reflux, at which point all solid went into solution. The solution was allowed to reflux for 24 h and then was cooled and filtered. The filtered out solid was taken up in a minimum volume of CHCl_3 , and the solution was passed through a neutral alumina column with CHCl_3 as the eluting solvent. The fastest moving orange band was collected, the solvent was removed by rotary evaporation, and precipitation was induced by the addition of methanol. Yield: 10.6 g (26%). Anal. Calc for $\text{C}_{22}\text{H}_{34}\text{N}_4\text{O}_2\text{Ni}$: C, 59.30; H, 7.70; N, 12.58. Found: C, 59.03; H, 7.83; N, 12.53.

(2,12,15,15-Tetramethyl-1,5,9,13-tetraazacyclohexadeca-1,4,9,12-tetraenoato- $\kappa^4\text{N}$)-nickel(II) Hexafluorophosphate, $[\text{NiDM}(\text{H}_2\text{Me}_2[16]\text{tetraeneN}_4)](\text{PF}_6)_2$. $\text{NiDM}(\text{Ac}_2\text{Me}_2[16]\text{tetraeneatoN}_4)$ (7.8 g, 18.7 mmol) was slurried in 75 mL of methanol, and 7.5 g of *p*-toluenesulfonic acid (39.4 mmol) was added. The mixture was heated to reflux for 5 min, 6.7 g of NH_4PF_6 in 20 mL of water was added, and the reaction was cooled in a freezer. The yellow microcrystalline product was filtered out and washed with methanol. Yield: 9.1 g (78%).

(2,7,12,15,15-Hexamethyl-1,5,9,13-tetraazacyclohexadeca-1,4,9,12-tetraenoato- $\kappa^4\text{N}$)-nickel(II) Hexafluorophosphate, $[\text{DMNiDM}(\text{H}_2\text{Me}_2[16]\text{tetraeneN}_4)](\text{PF}_6)_2$. This complex was synthesized in a manner analogous to that described for $[\text{NiDM}(\text{H}_2\text{Me}_2[16]\text{tetraeneN}_4)](\text{PF}_6)_2$, using 3.0 g of $\text{DMNiDM}(\text{Ac}_2\text{Me}_2[16]\text{tetraeneatoN}_4)$ (6.7 mmol), 2.7 g of *p*-toluenesulfonic acid, and 2.4 g of NH_4PF_6 . Yield: 3.2 g (73%).

(2,12,15,15-Tetramethyl-1,5,9,13-tetraazacyclohexadeca-1,3,9,11-tetraenoato- $\kappa^4\text{N}$)-nickel(II), $\text{NiDM}(\text{Me}_2[16]\text{tetraenoatoN}_4)$. To a solution of methanolic NaOCH_3 (0.8 g of Na (35 mmol) in 40 mL of methanol) was added 9.0 g of $[\text{NiDM}(\text{H}_2\text{Me}_2[16]\text{tetraeneN}_4)](\text{PF}_6)_2$ (14.4 mmol). The reaction immediately turned purple and was allowed to stir for 10 min. After the mixture was cooled in a freezer for 1 h, the dark purple solid was filtered out and dried in vacuo. Yield: 4.6 g (96%). This complex was used immediately in subsequent syntheses.

(25) (a) Evans, D. F. *J. Chem. Soc.* 1959, 2003. (b) Deutsch, J. L.; Poling, S. M. *J. Chem. Educ.* 1969, 46, 167. (c) Lolinger, J.; Scheffold, R. *J. Chem. Educ.* 1972, 49, 646. (d) Ostfeld, D.; Cohen, I. A. *J. Chem. Educ.* 1972, 49, 829.
(26) Drago, R. S. *Physical Methods in Chemistry*; Saunders: Philadelphia, PA, 1977.

(27) Riley, D. P.; Busch, D. H. *Inorg. Synth.* 1978, 18, 36.

(2,7,7,12,15,15-Hexamethyl-1,5,9,13-tetraazacyclohexadeca-1,3,9,11-tetraeneato- κ^4 N)nickel(II), $\text{DMNiDM}(\text{Me}_2[16]\text{tetraeneatoN}_4)$. This complex was synthesized in a manner analogous to that described for $\text{NiDM}(\text{Me}_2[16]\text{tetraeneatoN}_4)$, using 3.2 g of $[\text{DMNiDM}(\text{H}_2\text{Me}_2[16]\text{tetraeneatoN}_4)](\text{PF}_6)_2$ (4.9 mmol) and 0.27 g of Na metal. A moss green solid was obtained, which was determined to be the expected product by ^{13}C NMR spectroscopy. Yield: 1.6 g (91%).

(3,11-Dibenzoyl-2,7,7,12,15,15-tetramethyl-1,5,9,13-tetraazacyclohexadeca-1,3,9,11-tetraeneato- κ^4 N)nickel(II), $\text{NiDM}(\text{PhAc}_2\text{Me}_2[16]\text{tetraeneatoN}_4)$. $\text{NiDM}(\text{Me}_2[16]\text{tetraeneatoN}_4)$ (4.6 g, 13.8 mmol) was dissolved in 350 mL of diethyl ether, and 4.6 mL of triethylamine (2.4 equiv) was added. Benzoyl chloride (4.3 g, 2.2 equiv) was slowly dripped into the solution, resulting in an immediate orange precipitate. The solid was filtered out, washed with water, and redissolved in CHCl_3 . This solution was passed through a neutral alumina column with CHCl_3 as the eluent, collecting the fastest moving orange band. The solution volume was reduced to 10 mL, and ethanol was added to produce an orange solid. The product was washed with ethanol and dried in vacuo. Yield: 6.9 g (92%). Anal. Calc for $\text{C}_{30}\text{H}_{34}\text{N}_4\text{O}_2\text{Ni}$: C, 66.56; H, 6.33; N, 10.35. Found: C, 67.10; H, 5.84; N, 10.88.

(3,11-Dibenzoyl-2,7,7,12,15,15-hexamethyl-1,5,9,13-tetraazacyclohexadeca-1,3,9,11-tetraeneato- κ^4 N)nickel(II), $\text{DMNiDM}(\text{PhAc}_2\text{Me}_2[16]\text{tetraeneatoN}_4)$. This complex was synthesized in a manner analogous to that described in the previous reaction, using 1.5 g of $\text{DMNiDM}(\text{Me}_2[16]\text{tetraeneatoN}_4)$ (4.2 mmol), 1.5 g of triethylamine, and 1.3 g (2.2 equiv) of benzylamine. The peach precipitate was dissolved in CHCl_3 and loaded onto a neutral alumina column. A fast moving green band was eluted by using acetone and discarded, and the fastest moving orange band was collected upon elution with chloroform. The solvent volume of this fraction was reduced, and the addition of acetone induced the formation of long fine orange needles. Yield: 1.5 g (63%). Anal. Calc for $\text{C}_{32}\text{H}_{38}\text{N}_4\text{O}_2\text{Ni}$: C, 67.50; H, 7.21; N, 9.84. Found: C, 67.39; H, 7.09; N, 9.75.

(3,11-Bis(1-methoxyethylidene)-2,7,7,12-tetramethyl-1,5,9,13-tetraazacyclohexadeca-1,4,9,12-tetraene- κ^4 N)nickel(II) Hexafluorophosphate, $[\text{DMNi}(\text{MeOEtH}_2\text{Me}_2[16]\text{tetraeneatoN}_4)](\text{PF}_6)_2$. This complex was synthesized by the published method¹² with 10 g of methyl trifluoromethanesulfonate (57.5 mmol) as described by Novotnak²⁸ and 10.2 g of $\text{DMNi}(\text{Ac}_2\text{Me}_2[16]\text{tetraeneatoN}_4)$ (24.4 mmol). Upon removal of solvent a green precipitate formed, which was identified as the trifluoromethanesulfonate (triflate) salt by IR and ^{13}C NMR spectroscopy. This solid could be converted to the PF_6 salt by dissolving it in a small amount of methanol and slowly dripping in a 50-mL solution of 15.0 g of NH_4PF_6 in methanol. The resulting green powder was recrystallized from acetonitrile/methanol. Yield: 14.7 g (84%). Anal. Calc for $\text{C}_{22}\text{H}_{36}\text{N}_4\text{O}_2\text{NiP}_2\text{F}_{12}$: C, 35.84; H, 4.92; N, 7.60. Found: C, 35.66; H, 4.58; N, 7.56. ^{13}C NMR: 180.5, 173.6, 164.9, 67.9, 58.2, 51.4, 35.1, 29.0, 22.3, 15.9 ppm.

(3,11-Bis(1-methoxyethylidene)-2,12,15,15-tetramethyl-1,5,9,13-tetraazacyclohexadeca-1,4,9,12-tetraene- κ^4 N)nickel(II) Hexafluorophosphate, $[\text{NiDM}(\text{MeOEtH}_2\text{Me}_2[16]\text{tetraeneatoN}_4)](\text{PF}_6)_2$. This complex was synthesized as described in the previous reaction, using 8.0 g of $\text{NiDM}(\text{Ac}_2\text{Me}_2[16]\text{tetraeneatoN}_4)$ (19.2 mmol) and 10.0 g of methyl triflate. Yield: 5.0 g (35%). Anal. Calc for $\text{C}_{22}\text{H}_{36}\text{N}_4\text{O}_2\text{NiP}_2\text{F}_{12}$: C, 35.84; H, 4.92; N, 7.60. Found: C, 35.96; H, 4.88; N, 7.27. ^{13}C NMR: 173.5, 164.2, 118.0, 57.9, 57.3, 51.4, 35.8, 29.9, 25.9, 22.4, 15.7 ppm.

(3,11-Bis(1-methoxyethylidene)-2,7,7,12,15,15-hexamethyl-1,5,9,13-tetraazacyclohexadeca-1,4,9,12-tetraene- κ^4 N)nickel(II) Hexafluorophosphate, $[\text{DMNiDM}(\text{MeOEtH}_2\text{Me}_2[16]\text{tetraeneatoN}_4)](\text{PF}_6)_2$. This complex was synthesized as described in the previous reaction, using 10.2 g of $\text{DMNiDM}(\text{Ac}_2\text{Me}_2[16]\text{tetraeneatoN}_4)$ (22.9 mmol) and 10.0 g of methyl triflate. Yield: 16.3 g (93%). Anal. Calc for $\text{C}_{24}\text{H}_{40}\text{N}_4\text{O}_2\text{NiP}_2\text{F}_{12}$: C, 37.82; H, 5.29; N, 7.35. Found: C, 37.45; H, 4.98; N, 7.56. ^{13}C NMR: 180.3, 173.7, 165.0, 68.6, 61.3, 58.1, 35.9, 35.2, 25.9, 22.5, 15.8 ppm.

(3,11-Bis(α -methoxybenzylidene)-2,12,15,15-tetramethyl-1,5,9,13-tetraazacyclohexadeca-1,4,9,12-tetraene- κ^4 N)nickel(II) Hexafluorophosphate, $[\text{NiDM}(\text{MeOBenz}_2\text{Me}_2[16]\text{tetraeneatoN}_4)](\text{PF}_6)_2$. This complex was synthesized as described in the previous reaction, using 6.5 g of $\text{NiDM}(\text{PhAc}_2\text{Me}_2[16]\text{tetraeneatoN}_4)$ (12.0 mmol) and 4.9 g of methyl triflate. No triflate salt was obtained. Yield: 7.4 g (72%). Anal. Calc for $\text{C}_{32}\text{H}_{40}\text{N}_4\text{O}_2\text{NiP}_2\text{F}_{12}$: C, 44.62; H, 4.68; N, 6.50. Found: C, 45.01; H, 4.68; N, 6.56. ^{13}C NMR: 178.3, 174.1, 132.9, 130.5, 130.3, 130.1, 120.1, 61.6, 60.7, 57.1, 36.3, 30.2, 25.9, 23.1 ppm.

(3,11-Bis(α -methoxybenzylidene)-2,7,7,12,15,15-hexamethyl-1,5,9,13-tetraazacyclohexadeca-1,4,9,12-tetraene- κ^4 N)nickel(II) Hexafluorophosphate, $[\text{DMNiDM}(\text{MeOBenz}_2\text{Me}_2[16]\text{tetraeneatoN}_4)](\text{PF}_6)_2$.

This complex was synthesized as described in the previous reaction, using 1.4 g of $\text{DMNiDM}(\text{PhAc}_2\text{Me}_2[16]\text{tetraeneatoN}_4)$ (2.5 mmol) and 1.45 g of methyl triflate. Yield: 1.3 g (58%). Anal. Calc for $\text{C}_{34}\text{H}_{44}\text{N}_4\text{O}_2\text{NiP}_2\text{F}_{12}$: C, 45.91; H, 4.99; N, 6.30. Found: C, 45.61; H, 4.67; N, 6.16. ^{13}C NMR: 178.0, 173.8, 168.3, 132.5, 130.4, 130.0, 129.8, 119.3, 68.9, 61.2, 60.1, 35.8, 25.6, 22.1 ppm.

(2,7,7,12-Tetramethyl-3,11-bis[1-(methylamino)ethylidene]-1,5,9,13-tetraazacyclohexadeca-1,4,9,12-tetraene- κ^4 N)nickel(II) Hexafluorophosphate, $[\text{DMNi}(\text{Me}_2\text{Me}_2\text{H}_2[16]\text{cyclidene})](\text{PF}_6)_2$. Synthesis of this complex was accomplished by using the method of Schammel,²⁹ with 6.7 g of $[\text{NiDM}(\text{MeOEtH}_2\text{Me}_2[16]\text{tetraeneatoN}_4)](\text{PF}_6)_2$ (9.1 mmol), 5.9 g of methylamine hydrochloride (10 equiv), and 12.2 mL of triethylamine. Yield: 4.2 g (63%). Anal. Calc for $\text{C}_{28}\text{H}_{38}\text{N}_6\text{NiP}_2\text{F}_{12}$: C, 35.94; H, 5.21; N, 11.43. Found: C, 35.63; H, 4.87; N, 11.14. ^{13}C NMR: 169.6, 168.4, 159.7, 112.6, 68.2, 51.6, 36.2, 31.4, 30.7, 23.2, 20.8, 15.3 ppm.

(2,12,15,15-Tetramethyl-3,11-bis[1-(methylamino)ethylidene]-1,5,9,13-tetraazacyclohexadeca-1,4,9,12-tetraene- κ^4 N)nickel(II) Hexafluorophosphate, $[\text{NiDM}(\text{Me}_2\text{Me}_2\text{H}_2[16]\text{cyclidene})](\text{PF}_6)_2$. This complex was synthesized according to the previous synthesis, using 6.7 g of $[\text{NiDM}(\text{MeOEtH}_2\text{Me}_2[16]\text{tetraeneatoN}_4)](\text{PF}_6)_2$ (9.1 mmol), 5.9 g of methylamine hydrochloride (10 equiv), and 12.2 mL of triethylamine. Yield: 3.2 g (44%). Anal. Calc for $\text{C}_{28}\text{H}_{38}\text{N}_6\text{NiP}_2\text{F}_{12}$: C, 35.94; H, 5.21; N, 11.43. Found: C, 35.44; H, 4.99; N, 11.44. ^{13}C NMR: 169.4, 168.2, 159.6, 112.8, 61.5, 56.4, 36.0, 31.5, 30.4, 26.2, 20.7, 15.3 ppm.

(2,7,7,12,15,15-Hexamethyl-3,11-bis[1-(methylamino)ethylidene]-1,5,9,13-tetraazacyclohexadeca-1,4,9,12-tetraene- κ^4 N)nickel(II) Hexafluorophosphate, $[\text{DMNiDM}(\text{Me}_2\text{Me}_2\text{H}_2[16]\text{cyclidene})](\text{PF}_6)_2$. This complex was synthesized according to the previous synthesis, using 8.0 g of $[\text{DMNiDM}(\text{MeOEtH}_2\text{Me}_2[16]\text{tetraeneatoN}_4)](\text{PF}_6)_2$ (10.5 mmol), 8.0 g of methylamine hydrochloride (10 equiv), and 5 mL of triethylamine. Yield: 6.9 g (86%). Anal. Calc for $\text{C}_{24}\text{H}_{42}\text{N}_6\text{NiP}_2\text{F}_{12}$: C, 37.77; H, 5.55; N, 11.01. Found: C, 37.71; H, 6.11; N, 11.11. ^{13}C NMR: 169.7, 168.6, 159.8, 68.0, 61.4, 36.0, 35.0, 31.4, 26.2, 23.0, 21.0, 15.2 ppm.

(2,12,15,15-Tetramethyl-3,11-bis[α -(benzylamino)benzylidene]-1,5,9,13-tetraazacyclohexadeca-1,4,9,12-tetraene- κ^4 N)nickel(II) Hexafluorophosphate, $[\text{NiDM}(\text{Ph}_2\text{Bz}_2\text{H}_2[16]\text{cyclidene})](\text{PF}_6)_2$. Synthesis of this complex was accomplished by using the method of Schammel,²⁹ using 3.0 g of $\text{NiDM}(\text{PhAc}_2\text{Me}_2[16]\text{tetraeneatoN}_4)$ (3.5 mmol) and 0.8 g (7.5 mmol) of benzylamine. Yield: 2.8 g (79%). Anal. Calc for $\text{C}_{44}\text{H}_{50}\text{N}_6\text{NiP}_2\text{F}_{12}$: C, 52.24; H, 4.98; N, 8.31. Found: C, 52.77; H, 4.80; N, 7.89. ^{13}C NMR: 169.5, 162.8, 137.2, 131.3, 130.9, 130.2, 129.9, 129.3, 61.7, 56.4, 36.3, 30.2, 26.3, 21.2 ppm.

(2,7,7,12,15,15-Hexamethyl-3,11-bis[α -(benzylamino)benzylidene]-1,5,9,13-tetraazacyclohexadeca-1,4,9,12-tetraene- κ^4 N)nickel(II) Hexafluorophosphate, $[\text{DMNiDM}(\text{Ph}_2\text{Bz}_2\text{H}_2[16]\text{cyclidene})](\text{PF}_6)_2$. This complex was synthesized according to the previous synthesis, using 1.3 g of $\text{DMNiDM}(\text{PhAc}_2\text{Me}_2[16]\text{tetraeneatoN}_4)$ (1.5 mmol) and 0.5 g (3 equiv) of benzylamine. No solid was isolated; the oily product was utilized directly in the subsequent synthesis.

Synthesis of Bridged Nickel(II) Complexes. (2,3,11,12,14,20,24,24-Octamethyl-3,11,15,19,22,26-hexaazatricyclo[11.7.7.1^{5,9}]octacos-1,5,7,9(28),12,14,19,21,26-nonaene- κ^4 N)nickel(II) Hexafluorophosphate, $[\text{DMNi}(\text{Me}_2\text{Me}_2\text{Mxy}[16]\text{cyclidene})](\text{PF}_6)_2$. This complex was synthesized according to published procedures.¹²

(2,3,11,12,14,17,17,20-Octamethyl-3,11,15,19,22,26-hexaazatricyclo[11.7.7.1^{5,9}]octacos-1,5,7,9(28),12,14,19,21,26-nonaene- κ^4 N)nickel(II) Hexafluorophosphate, $[\text{NiDM}(\text{Me}_2\text{Me}_2\text{Mxy}[16]\text{cyclidene})](\text{PF}_6)_2$. This compound was synthesized according to published procedures,³⁰ using $[\text{NiDM}(\text{Me}_2\text{Me}_2\text{H}_2[16]\text{cyclidene})](\text{PF}_6)_2$ (4.0 g, 5.5 mmol) in 240 mL of acetonitrile, 0.26 g of sodium (11.3 mmol), and 1.45 g of α,α -dibromo-*m*-xylene (5.5 mmol). Yield: 2.6 g (56%). Anal. Calc for $\text{C}_{30}\text{H}_{44}\text{N}_6\text{NiP}_2\text{F}_{12}\text{CH}_3\text{CN}$: C, 43.76; H, 5.39; N, 11.16. Found: C, 43.74; H, 5.49; N, 11.11.

(2,3,11,12,14,17,17,20,24,24-Decamethyl-3,11,15,19,22,26-hexaazatricyclo[11.7.7.1^{5,9}]octacos-1,5,7,9(28),12,14,19,21,26-nonaene- κ^4 N)nickel(II) Hexafluorophosphate, $[\text{DMNiDM}(\text{Me}_2\text{Me}_2\text{Mxy}[16]\text{cyclidene})](\text{PF}_6)_2$. This complex was synthesized in the manner described above, using 4.2 g of $[\text{DMNiDM}(\text{Me}_2\text{Me}_2\text{H}_2[16]\text{cyclidene})](\text{PF}_6)_2$ (5.5 mmol), 0.29 g of Na, and 1.45 g of α,α -dibromo-*m*-xylene. Yield: 3.1 g (65%). Anal. Calc for $\text{C}_{32}\text{H}_{48}\text{N}_6\text{NiP}_2\text{F}_{12}\text{CH}_3\text{CN}$: C, 45.09; H, 5.67; N, 10.81. Found: C, 45.09; H, 5.85; N, 11.00.

(3,11-Dibenzyl-14,17,17,20-tetramethyl-2,12-diphenyl-3,11,15,19,22,26-hexaazatricyclo[11.7.7.1^{5,9}]octacos-1,5,7,9-

(28) Novotnak, G. C. Ph.D. Thesis, The Ohio State University, 1988.

(29) Schammel, W. P.; Zimmer, L. L.; Busch, D. H. *Inorg. Chem.* **1980**, *19*, 3159.

(30) Olszanski, D. J.; Stevens, J. C.; Schammel, W. P.; Kojima, M.; Herron, N.; Zimmer, L. L.; Holter, K. A.; Mocak, J.; Busch, D. H. *J. Am. Chem. Soc.* **1981**, *103*, 2421.

(28), 12, 14, 19, 21, 26-nonaene- κ^4N nickel(II) Hexafluorophosphate, [NiDM{Ph₂Bz₂Mxy}[16]cyclidene]}(PF₆)₂. This complex was synthesized in the manner described above, using 2.6 g of [NiDM{Ph₂Bz₂H₂[16]cyclidene]}(PF₆)₂ (2.6 mmol), 0.70 g of α,α -dibromo-*m*-xylene, and 0.13 g of Na metal. Following purification by column chromatography, the orange microcrystalline product was precipitated by reducing the solvent volume to 20 mL, adding ethanol until a cloudiness persisted, adding 50 mL of methanol, and chilling in a freezer for 1 h. Yield: 1.5 g (52%). Anal. Calc for C₄₂H₄₆N₆NiP₂F₁₂: C, 56.08; H, 5.07; N, 7.55. Found: C, 56.34; H, 5.49; N, 7.19. ¹³C NMR: 172.1, 168.0, 162.2, 137.3, 134.9, 133.6, 132.8, 131.9, 130.7, 130.3, 130.0, 129.6, 129.4, 128.1, 125.8, 115.6, 61.7, 61.3, 57.2, 56.4, 35.6, 26.0, 25.9, 20.7 ppm.

(3, 11-Dibenzyl-14, 17, 20, 24, 24-hexamethyl-2, 12-diphenyl-3, 11, 15, 19, 22, 26-hexaazatriacyclo[11.7.7.1^{5,9}]octacos-1, 5, 7, 9-(28), 12, 14, 19, 21, 26-nonaene- κ^4N nickel(II) Hexafluorophosphate, [DMNiDM{Ph₂Bz₂Mxy}[16]cyclidene]}(PF₆)₂. This complex was produced by the method described in the previous synthesis, using 0.9 g of [DMNiDM{Ph₂Bz₂H₂[16]cyclidene]}(PF₆)₂ (0.87 mmol), 0.24 g of α,α -dibromo-*m*-xylene, and 0.05 g of Na metal. Yield: 0.87 g (96%). Anal. Calc for C₅₄H₆₀N₆NiP₂F₁₂: C, 56.81; H, 5.30; N, 7.36. Found: C, 56.72; H, 5.31; N, 7.27. ¹³C NMR: 172.8, 167.9, 162.6, 137.4, 135.1, 133.9, 133.4, 132.2, 131.0, 130.8, 130.7, 130.5, 130.1, 130.0, 128.0, 125.8, 116.0, 69.3, 62.2, 61.6, 57.8, 35.8, 33.7, 26.4, 26.0, 24.5, 21.2, 19.2 ppm.

2, 3, 11, 12, 14, 20, 24-Octamethyl-3, 11, 15, 19, 22, 26-hexaazatriacyclo[11.7.7.1^{5,9}]octacos-1, 5, 7, 9-(28), 12, 14, 19, 21, 26-nonaene Bromide Hexafluorophosphate, [DMH₄{Me₂Me₂Mxy}[16]cyclidene]}Br(PF₆)₃. [DMNi{Me₂Me₂Mxy}[16]cyclidene]}(PF₆)₂ (1.0 g, 1.2 mmol) was slurried in 30 mL of methanol. Hydrogen bromide gas was bubbled vigorously through the mixture. After 1 min, the solid was completely dissolved, and the solution color changed from orange to bright green after 5 min. The HBr bubbling continued for another 15 min, and the solvent was completely removed by rotary evaporation, leaving a cream colored solid and a green oil. A 10-mL portion of water was added, dissolving all solids, and 1.0 g of NH₄PF₆ in 10 mL of water was slowly dripped into the solution. The cream colored product was filtered out, washed with water and diethyl ether, and dried in vacuo. Yield: 0.8 g (68%).

2, 3, 11, 12, 14, 17, 20-Octamethyl-3, 11, 15, 19, 22, 26-hexaazatriacyclo[11.7.7.1^{5,9}]octacos-1, 5, 7, 9-(28), 12, 14, 19, 21, 26-nonaene Bromide Hexafluorophosphate, [H₄DM{Me₂Me₂Mxy}[16]cyclidene]}Br(PF₆)₃; 2, 3, 11, 12, 14, 17, 20, 24, 24-Decamethyl-3, 11, 15, 19, 22, 26-hexaazatriacyclo[11.7.7.1^{5,9}]octacos-1, 5, 7, 9-(28), 12, 14, 19, 21, 26-nonaene Bromide Hexafluorophosphate, [DMH₄DM{Me₂Me₂Mxy}[16]cyclidene]}Br(PF₆)₃; 3, 11-Dibenzyl-14, 17, 20-tetramethyl-2, 12-diphenyl-3, 11, 15, 19, 22, 26-hexaazatriacyclo[11.7.7.1^{5,9}]octacos-1, 5, 7, 9-(28), 12, 14, 19, 21, 26-nonaene Bromide Hexafluorophosphate, [H₄DM{Ph₂Bz₂Mxy}[16]cyclidene]}Br(PF₆)₃; 3, 11-Dibenzyl-14, 17, 20, 24, 24-hexamethyl-2, 12-diphenyl-3, 11, 15, 19, 22, 26-hexaazatriacyclo[11.7.7.1^{5,9}]octacos-1, 5, 7, 9-(28)-12, 14, 19, 21, 26-nonaene Bromide Hexafluorophosphate, [DMH₄DM{Ph₂Bz₂Mxy}[16]cyclidene]}Br(PF₆)₃. These compounds were synthesized by the above procedure with yields generally between 60 and 90%.

Synthesis of Iron(II) Complexes. (2, 3, 11, 12, 14, 20, 24-Octamethyl-3, 11, 15, 19, 22, 26-hexaazatriacyclo[11.7.7.1^{5,9}]octacos-1, 5, 7, 9-(28), 12, 14, 19, 21, 26-nonaene- κ^4N)iron(II) Hexafluorophosphate, [DMFe{Me₂Me₂Mxy}[16]cyclidene]}(PF₆)₂. To a slurry of 0.26 g of [DMH{Me₂Me₂Mxy}[16]cyclidene]}Br(PF₆)₃ (0.26 mmol) and 0.12 g of bis(pyridine)iron(II) dichloride (0.42 mmol) in 10 mL of acetonitrile was added 0.3 mL of triethylamine. The resulting deep red solution was heated to boiling for 5 min and then cooled to room temperature. The reaction was then filtered and the solvent removed from the filtrate. The red oil was redissolved in hot ethanol, and the solution was allowed to cool, causing a red precipitate to form. The solid was filtered out and washed with a small amount of ethanol. Further reduction of the filtrate resulted in the formation of additional product. Yield: 0.18 g (79%). Anal. Calc for C₃₀H₄₄N₆FeClP₂F₆: C, 49.70; H, 6.12; N, 11.59; Fe, 7.70. Found: C, 49.45; H, 6.14; N, 11.26; Fe, 7.26.

(2, 3, 11, 12, 14, 17, 20-Octamethyl-3, 11, 15, 19, 22, 26-hexaazatriacyclo[11.7.7.1^{5,9}]octacos-1, 5, 7, 9-(28), 12, 14, 19, 21, 26-nonaene- κ^4N)iron(II) Hexafluorophosphate, [FeDM{Me₂Me₂Mxy}[16]cyclidene]}(PF₆)₂. This complex was obtained in the same manner as described for the preceding reaction, using 0.40 g of [H₄DM{Me₂Me₂Mxy}[16]cyclidene]}Br(PF₆)₃ (0.40 mmol), 0.12 g of bis(pyridine)iron(II) chloride (0.42 mmol), and 0.23 mL of triethylamine. An ethanolic solution of NH₄PF₆ was added to obtain additional product. Yield: 0.17 g (59%). Anal. Calc for C₃₀H₄₄N₆FeP₂F₁₂-CH₃CN: C, 43.90; H, 5.41; N, 11.20; Fe, 6.38. Found: C, 43.51; H, 4.99; N, 10.77; Fe, 5.79.

(2, 3, 11, 12, 14, 17, 20, 24, 24-Decamethyl-3, 11, 15, 19, 22, 26-hexaazatriacyclo[11.7.7.1^{5,9}]octacos-1, 5, 7, 9-(28), 12, 14, 19, 21, 26-nonaene- κ^4N)iron(II) Hexafluorophosphate, [DMFeDM{Me₂Me₂Mxy}[16]cyclidene]}(PF₆)₂. This complex was synthesized as described for the previous reaction, using 0.27 g of [DMH₄DM{Me₂Me₂Mxy}[16]cyclidene]}Br-

(PF₆)₃ (0.27 mmol), 0.12 g of bis(pyridine)iron(II) chloride, and 0.3 mL of triethylamine. Yield: 0.10 g (50%). Anal. Calc for C₃₂H₄₈N₆FeP₂F₁₂-CH₃CN: C, 45.19; H, 5.69; N, 10.85; Fe, 6.18. Found: C, 44.95; H, 5.24; N, 10.26; Fe, 5.46.

(3, 11-Dibenzyl-14, 20, 24, 24-tetramethyl-2, 12-diphenyl-3, 11, 15, 19, 22, 26-hexaazatriacyclo[11.7.7.1^{5,9}]octacos-1, 5, 7, 9-(28), 12, 14, 19, 21, 26-nonaene- κ^4N)iron(II) Hexafluorophosphate, [DMFe{Ph₂Bz₂Mxy}[16]cyclidene]}(PF₆)₂. This complex was synthesized by the previous procedure and was provided by Dr. Lyndel Dickerson.

(3, 11-Dibenzyl-14, 17, 17, 20-tetramethyl-2, 12-diphenyl-3, 11, 15, 19, 22, 26-hexaazatriacyclo[11.7.7.1^{5,9}]octacos-1, 5, 7, 9-(28), 12, 14, 19, 21, 26-nonaene- κ^4N)iron(II) Hexafluorophosphate, [FeDM{Ph₂Bz₂Mxy}[16]cyclidene]}(PF₆)₂. To a solution of [H₄DM{Ph₂Bz₂Mxy}[16]cyclidene]}Br(PF₆)₃ (0.35 g, 0.29 mmol) in 10 mL of acetonitrile was added 0.10 g of bis(pyridine)iron(II) chloride (1.2 equiv) and 0.27 mL of triethylamine (4.1 equiv). The deep red solution was heated for 5 min and then was allowed to cool to room temperature. The solution was filtered through Celite and the solvent removed from the filtrate. The remaining red tar was dissolved in a minimum amount of hot ethanol, and after cooling, the dark red solid formed was filtered out, washed with a small amount of ethanol, and dried in vacuo. Yield: 1.5 g (45%). Anal. Calc for C₅₂H₅₆N₆FeClP₂F₆: C, 62.37; H, 5.64; N, 8.39; Fe, 5.58. Found: C, 62.01; H, 6.00; N, 8.01; Fe, 5.30.

(3, 11-Dibenzyl-14, 17, 17, 20, 24, 24-hexamethyl-2, 12-diphenyl-3, 11, 15, 19, 22, 26-hexaazatriacyclo[11.7.7.1^{5,9}]octacos-1, 5, 7, 9-(28), 12, 14, 19, 21, 26-nonaene- κ^4N)iron(II) Hexafluorophosphate, [DMFeDM{Ph₂Bz₂Mxy}[16]cyclidene]}(PF₆)₂. This complex was prepared by using the procedure described in the preceding synthesis, using 0.60 g of [DMH₄DM{Ph₂Bz₂Mxy}[16]cyclidene]}Br(PF₆)₃ (0.46 mmol), 0.15 g of bis(pyridine)iron(II) chloride (1.1 equiv), and 0.26 mL of triethylamine. Yield: 0.28 g (59%). Anal. Calc for C₅₄H₆₀N₆FeClP₂F₆: C, 63.01; H, 5.88; N, 8.16; Fe, 5.39; Cl, 3.44. Found: C, 62.75; H, 5.88; N, 7.95; Fe, 5.30; Cl, 3.41.

X-ray Structure Determination. The crystal structure was determined for [DMNiDM{Me₂Me₂Mxy}[16]cyclidene]}(PF₆)₂ by X-ray diffraction methods. Relevant data are listed in Table I. Data were collected with a Syntex P2₁ diffractometer in the $\theta/2\theta$ mode. Maximum 2θ was 45° with scan range $\pm 1.1^\circ - 2\theta$ about the $K\alpha_1 - K\alpha_2$ positions; scan speed was 2–28° min⁻¹. Backgrounds were measured at each end of the scan for 0.25 of the scan time. *hkl* ranges: 0/25; 0/18; 25/25. Unit cell dimensions and standard deviations were obtained by a least-squares fit to 15 reflections (20 < 2θ < 22°). Reflections were processed by using a profile analysis to give 5240 unique reflections ($R_{int} = 0.025$); 3302 were considered observed ($1/\sigma(I) \geq 2.0$) and were corrected for Lorentz, polarization, and absorption effects, the latter by the Gaussian method with maximum and minimum transmission factors of 0.939 and 0.876. Crystal size: 0.18 × 0.48 × 0.91 mm. Three standard reflections were monitored every 200 reflections and showed slight fluctuations during data collection, corrected by a moving rescale procedure.

Systematic absences $h0l$, $l = 2n$, and $0k0$, $k = 2n$, indicate that the space group is $P2_1/c$.

The structure was solved by first locating the nickel atom from a Patterson map, and the remaining non-hydrogen atoms were then found on successive Fourier syntheses, including a disordered acetonitrile solvent molecule. Anisotropic temperature factors were used for all non-hydrogen atoms. One PF₆ group was disordered and was approximated by nine fluorine atoms each at 0.5 occupancy. Hydrogen atoms were given fixed isotropic temperature factors and inserted at calculated positions without refinement; methyl groups were treated as rigid CH₃ units with their initial orientations taken from the strongest peaks on the difference Fourier synthesis. Final refinement was on F by cascaded least-squares methods, refining 534 parameters. Largest residual peaks were of height +1.1 and -0.04 e Å⁻³, all near the disordered solvent or PF₆ groups. A weighting scheme of the form $W = 1/((S(F)^2 + gF^2))$ with $g = 0.00354$ was used and shown to be satisfactory by a weight analysis. Final $R = 0.083$ and $R_w = 0.091$; such relatively high values are often found with this class of compounds and are not unexpected in the presence of disordered solvent and ions. Computing was with SHEXTL³¹ on a Data General DG30 computer, and scattering factors in the analytical form and anomalous dispersion factors were taken from ref 32. Final atomic coordinates are listed in supplementary material Table S4.

Acknowledgment. Support of this research by the National Science Foundation, Grant No. CHE 8822822, and the National Institutes of Health, Grant No. GM 10040, is gratefully ac-

(31) Sheldrick, G. M. *SHEXTL PLUS: User's Manual*; Nicolet Instrument Co.: Madison, WI, 1986.

(32) *International Tables for X-ray Crystallography*; Kynoch: Birmingham, England, 1974; Vol. IV.

knowledge. The collaboration between The Ohio State University and the University of Warwick has been supported by a NATO travel grant.

Supplementary Material Available: Tables S1-S8, listing selected

infrared bands, NMR chemical shift values, atomic coordinates, bond lengths, bond angles, anisotropic thermal parameters, and H atom coordinates and temperature factors (9 pages); Table S9, listing structure factors (8 pages). Ordering information is given on any current masthead page.

Contribution from the Chemistry Department,
The Ohio State University, Columbus, Ohio 43210

Synthesis, Electron Spin Resonance Spectroscopy, and Shape-Determining Angle Analysis of Superstructured Copper(II) Schiff Base Complexes Containing Persistent Voids

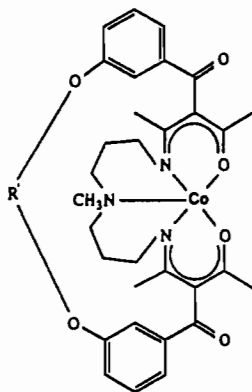
William M. Davis, Sharlene J. Dzigan, Mark W. Glogowski, Rita Delgado, and Daryle H. Busch*

Received June 15, 1990

Syntheses, electron spin resonance spectroscopy, X-ray structural determinations, and shape-determining angle analyses for the five-coordinate Schiff base complexes [Cu(Me₂H₂Me₂malMeDPT)], [Cu{Me₂(C3)Me₂malMeDPT}], and [Cu{Me₂(C6)Me₂malMeDPT}] are reported. Syntheses of the superstructured complexes are accomplished by utilizing high-dilution techniques. Interpretation of the ESR spectra suggests that the complexes are five-coordinate with geometries intermediate between TBP and SP. This interpretation is supported by the X-ray structure of each complex. [Cu(Me₂H₂Me₂malMeDPT)] crystallizes in the monoclinic system (*C2/c*) with unit cell dimensions $a = 17.746$ (3) Å, $b = 7.108$ (1) Å, $c = 17.278$ (2) Å, $\beta = 121.68$ (1)°, and $Z = 4$. A total of 2046 reflections were collected, 1662 with $I > 3\sigma(I)$. The structure was refined to weighted and unweighted R factors of 4.2 and 4.0%, respectively. [Cu{Me₂(C3)Me₂malMeDPT}] crystallizes in the orthorhombic system (*Pbca*) with unit cell dimensions $a = 9.758$ (1) Å, $b = 35.922$ (2) Å, and $c = 17.899$ (2) Å. With 2960 reflections having intensities greater than $3\sigma(I)$, the structure was refined to weighted and unweighted R factors of 6.0 and 5.2%, respectively. [Cu{Me₂(C6)Me₂malMeDPT}] crystallizes in the triclinic system (*P1*) with unit cell dimensions $a = 11.437$ (1) Å, $b = 13.374$ (1) Å, $c = 13.611$ Å, $\alpha = 101.02$ (1)°, $\beta = 116.73$ (1)°, and $\gamma = 101.14$ (1)°. Weighted and unweighted R factors are 4.1 and 4.3%, respectively, for 3991 reflections with $I > 3\sigma(I)$.

Introduction

In a preliminary communication¹ we reported the successful design and synthesis of cobalt(II) dioxygen carriers of the structure I. Central to this work on dioxygen carriers is the principle of



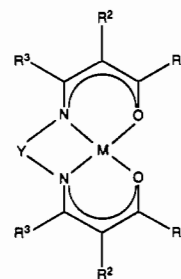
I

inclusion chemistry and the fundamental guest-host interaction of the O₂ molecule with the lacunar carrier complex.² The copper complexes that we report here serve as the direct precursors to the host cobalt complexes. Their structural analyses are important, not only in the designing ideal host molecules for dioxygen but also for demonstrating the ability to create structures with variable persistent voids.³

The complex [Cu(Me₂H₂Me₂malMeDPT)]⁴ was first prepared by Cummings et al.⁵ and was thoroughly characterized with the exception of an X-ray structural determination. The structure of this related unbridged complex (II in Scheme I) is reported herein for comparison to the superstructured copper complexes

(III in Scheme I). All three structures display coordination geometries about copper that are intermediate between trigonal bipyramidal (TBP) and square pyramidal (SP). Muettterties⁶ has refined a method for more precisely describing these intermediate geometries via reference to idealized polyhedra. These *shape-determining angles* about a coordination sphere define the mo-

- (1) Delgado, R.; Glogowski, M. W.; Busch, D. H. *J. Am. Chem. Soc.* **1987**, *109*, 6855.
- (2) (a) Busch, D. H.; Stephenson, N. A. *J. Inclusion Phenom. Recognit. Chem.* **1989**, *7*, 137. (b) Busch, D. H. *Synthetic Dioxygen Carriers for Dioxygen Transport*. In *Oxygen Complexes and Oxygen Activation by Transition Metals*; Martell, A. E., Sawyer, D. T., Eds.; Plenum Publishing Corp.: New York, 1988.
- (3) (a) Atwood, J. L.; Davies, J. E. D., Eds. *Inclusion Phenomena in Inorganic, Organic and Organometallic Hosts*; D. Reidel Publishing Co.: Boston, MA, 1987. (b) Meade, T. J.; Busch, D. H. In *Progress in Inorganic Chemistry*; Lippard, S. J., Ed.; Wiley: New York, 1985; Vol. 33, p 59. (c) Alcock, N. W.; Lin, W.-K.; Cairns, C.; Pike, G. A.; Busch, D. H. *J. Am. Chem. Soc.* **1989**, *111*, 6630.
- (4) We have chosen to name complexes of this type in a consistent manner (Goldsby, K. A.; Jircitano, A. J.; Minahan, D. M.; Ramprasad, D.; Busch, D. H. *Inorg. Chem.* **1987**, *26*, 2651) based on the structure



[M(R¹₂R²₂malY)]

- (5) Chen, Y.; Chu, D. E.; McKinney, B. D.; Willis, L. J.; Cummings, S. C. *Inorg. Chem.* **1981**, *20*, 1885, 3582.
- (6) Muettterties, E. L.; Guggenberger, L. J. *J. Am. Chem. Soc.* **1974**, *96*, 1748.

* To whom correspondence should be addressed at the Chemistry Department, The University of Kansas, Lawrence, KS 66045.